

بِسْمِ اللَّهِ الرَّحْمَنِ الرَّحِيمِ



Sudan University for Science and Technology

College Graduate Studies

Measurement of Normal Caudate Nucleus Dimensions in Magnetic Resonance Images for Sudanese Populationand

قياس النواة المذنبة الطبيعية لدى السودانيين باستخدام الرنين المغنطيسي

A thesis submitted for partial fulfillment for the requirement of M.Sc
degree In Radiological imaging diagnosis

Prepared by:-

Badraldeen Osman Gabir Ahmed

Supervised by:-

DR. Hussein Ahmed Hassan Ahmed

2016



الاية:-

قال تعالى:

{ اِقْرَأْ بِاسْمِ رَبِّكَ الَّذِي خَلَقَ (1) خَلَقَ
الْإِنْسَانَ مِنْ عَلَقٍ (2)

اِقْرَأْ وَرَبُّكَ الْأَكْرَمُ (3) الَّذِي عَلَّمَ
بِالْقَلَمِ (4) عَلَّمَ الْإِنْسَانَ مَا لَمْ

يَعْلَمُ (5) {
صدق الله العظيم

سورة العلق الآيات (1-5)

Abstract

this descriptive study was conducted at ROYAL care specialized hospital and AL zaytouna specialized hospital between 3/9/2016 to 29/11/2016 the was conducted on one hundred patient(50 males and 50 females) referred to radiology department for brain magnetic resonance imaging examination having no brain disorder that affect the caudate nucleus the study aimed to provide Sudanese index (dimension) for caudate nucleus (head ,body , tail) in normal population.

Because of the lack of studies for caudate nucleus measurements to determine the average range of caudate nucleus dimensions and measure the length and width of the caudate nucleus and compare between male and female caudate nucleus

The result noted that the mean for the length and width of the right and left head and body and tail of caudate nucleus for males and females. were Length in males of right head length of caudate nucleus (23.45 ± 2.54), right body length of caudate nucleus (18.18 ± 2.48), right tail length of caudate nucleus (9.60 ± 1.57), left head length of caudate nucleus (21.26 ± 2.27), left body length of caudate nucleus (16.40 ± 2.56), left tail length of caudate nucleus (8.34 ± 1.91), Width in males right head with of caudate nucleus (9.16 ± 1.49), right body width of caudate nucleus (7.18 ± 1.40), right tail width of caudate nucleus (4.31 ± 1.1), left head width of caudate nucleus (8.44 ± 1.40), left body width of caudate nucleus (6.58 ± 1.28), left tail width of caudate nucleus (3.82 ± 1.18)

Length in females right head length of caudate nucleus (22.61 ± 1.99), right body length of caudate nucleus (17.23 ± 22.12), right tail length of caudate nucleus (9.05 ± 1.75), left head length of caudate nucleus

(20.81 ± 2.18), left body length of caudate nucleus (15.79 ± 2.31), left tail length of caudate nucleus (7.84 ± 1.75), Width in females right head width of caudate nucleus (8.90 ± 1.28), right body width of caudate nucleus (7.10 ± 1.43), right tail width of caudate nucleus ($4.44 \pm .78$), left head width of caudate nucleus 8.48 ± 1.35 , left body width of caudate nucleus (6.55 ± 1.32), left tail width of caudate nucleus ($3.80 \pm .79$) In mm respectively

We concluded that According to the result the size of the caudate nucleus is higher in male than female except in left head width of caudate nucleus and right tail width of caudate nucleus was higher in females than in males

Further study in evaluation of caudate nucleus with larger sample of Sudanese population for more accurate results is needed

ملخص البحث

وقد أجريت هذه الدراسة الوصفية في مستشفى رويال كير المتخصصة و مستشفى الزيتونة المتخصصة في الفترة من 09/03/2016 إلى 2016/11/29 وأجريت على مائة مريض (50 من الذكور و 50 من الإناث) تم تحويلهم لقسم الأشعة لاجراء فحص التصوير بالرنين المغناطيسي لادمغتهم حيث انهم لا يعانون من اي اضطراب او امراض في الدماغ قد تؤثر على النواة المذنبة.

تهدف الدراسة الى توفير فهرس سوداني (البعد) لقياس النواة المذنبة (الرأس والجسم والذيل) لدى الاصحاء

ونظرا لعدم وجود دراسات لقياس المذنبة نواة لتحديد المدى المتوسط لأبعاد النواة المذنبة وقياس طول وعرض النواة المذنبة ومقارنة النواة المذنبة بين الذكور والإناث

وأشارت النتائج لانخفاض متوسط الطول والعرض في كلا من النواه المذنبة اليمنة واليسرة (الرأس و الجسم والذيل) للذكور والإناث. كان الطول في الذكور كالاتى طول الرأس الأيمن من المذنبة نواة (2.54 ± 23.45)، طول الجسم الأيمن من المذنبة نواة (2.48 ± 18.18)، وطول الذيل الأيمن من المذنبة نواة (1.57 ± 9.60)، في يسار طول الرأس النواة المذنبة (2.27 ± 21.26)، طول الجسم الايسر من النواة المذنبة (2.56 ± 16.40)، طول ذيل الايسر النواة المذنبة (1.91 ± 8.34)، العرض في الذكور كالاتى عرض الرأس الايمن من المذنبة نواة (1.49 ± 9.16)، عرض الجسم الأيمن من النواة المذنبة (1.40 ± 7.18)، عرض ذيل الأيمن من المذنبة نواة (1.1 ± 4.31) عرض الرأس الايسر المذنبة نواة (1.40 ± 8.44) عرض الجسم الايسر من المذنبة نواة (1.28 ± 6.58)، عرض ذيل الايسر المذنبة نواة (1.18 ± 3.82)

الطول في الإناث كالاتى طول الرأس الايمن من المذنبة نواة (1.99 ± 22.61)، طول الجسم الأيمن من المذنبة نواة (22.12 ± 17.2)، طول الذيل الأيمن من المذنبة نواة (9.05 ± 1.75)، طول الرأس الايسر النواة المذنبة (20.81 ± 2.18) طول الجسم الايسر من المذنبة نواة (2.31 ± 15.79)، طول ذيل الايسر النواة المذنبة (1.75 ± 7.84)، العرض في الإناث عرض الرأس الأيمن من المذنبة نواة (1.28 ± 8.90)، عرض الجسم الأيمن من نواة المذنبة

(7.10 +/- 1.43)، العرض ذيل الايمن المذنب نواة (4.44 ± 78)، عرض الراس الايسر من المذنبه نواة (8.48 +/- 1.35)، عرض الجسم الايسر من المذنبه نواة (6.55 ± 1.32)، عرض ذيل الايسر من المذنب نواة (3.80 ± 79) ملم على التوالي استنتجنا من هذه القياسات ان حجم النواة المذنبه أعلى في الذكور من الإناث إلا في عرض الراس الأيسر من النواة المذنبه وعرض ذيل الأيمن من نواة المذنب كانت أعلى لدى الإناث من الذكور وهناك حاجة إلى مزيد من الدراسات لتقييم النواة المذنبه في عينة أكبر من السودانيين للحصول على نتائج أكثر دقة

Dedication

*This humble work is dedicated
to my family and many friends*

Acknowledgments

*This thesis becomes a reality with the kind support and help of
many individuals.*

I would like to extend my sincere thanks to all of them

Foremost I want to offer this endeavor to Allah

*I would like to express my gratitude towards my family for
support which helped me*

CONTENTS

Topic	Page
الايه	I
Abstract English	II
Abstract Arabic	IV
Dedication	VI
Acknowledgment	VII
List of content	VIII
List of figures	X
List of tables	XIII
Abbreviation	XIV
Chapter one	
Introduction	1
Problem of study	2
Objectives	2
Chapter two	
Anatomy	4
physiology	9
Pathology	11

Previous study	27
Chapter three	
Material and methods	31
Chapter four	
Results	33
Chapter five	
Discussion	48
Conclusion	51
Recommendations	52
References	53
Appendices	

List of figures:

Fig Number	Name of figure	Page
2.1	Basal ganglia labeled at top right	5
2.2	Coronal slices show head of caudate nucleus	6
2.3	basal ganglia	8
2.4	Location of the substantianigra within the basal ganglia	9
4.1	1 A scatter plot diagram shows a linear relationship between the RTHL and the Age of the subjects, $R^2=0.083$.	34
4.2	A scatter plot diagram shows a linear relationship between the RTBL and the Age of the subjects, $R^2=0.026$.	34
4.3	A scatter plot diagram shows a linear relationship between the RTTL and the Age of the subjects, $R^2=0.004$.	35
4.4	A scatter plot diagram shows a linear relationship between the RTHW and the Age of the subjects, $R^2=0.108$.	35
4.5	A scatter plot diagram shows a linear relationship between the RTBW and the Age of the subjects, $R^2=0.094$	36
4.6	A scatter plot diagram shows a linear relationship between the RTTW and the Age of the subjects, $R^2=0.063$.	36

4.7	A scatter plot diagram shows a linear relationship between the LTHL and the Age of the subjects, $R^2=0.073$	37
4.8	A scatter plot diagram shows a linear relationship between the LTBL and the Age of the subjects, $R^2=0.025$	37
4.9	. A scatter plot diagram shows a linear relationship between the LTTL and the Age of the subjects, $R^2=0.003$.	38
4.10	A scatter plot diagram shows a linear relationship between the LTHW and the Age of the subjects, $R^2=0.028$	38
4.11	A scatter plot diagram shows a linear relationship between the LTBW and the Age of the subjects, $R^2=0.030$	39
4.12	A scatter plot diagram shows a linear relationship between the LTTW and the Age of the subjects, $R^2=0.01$.	39
4.13	comparison between males and females in mean Age	40
4.14	comparison between males and females in RTHL	41
4.15	comparison between males and females in RTBL	41
4.16	: comparison between males and females in RTTL	42
4.17	comparison between males and females in RTHW	42
4.18	comparison between males and females in RTBW	43
4.19	∴ comparison between males and females in RTTW	43
4.20	comparison between males and females in LTHL .	44
4.21	Comparison between male and female in LTBL	44
4.22	comparison between males and females in LTTL	45

4.23	comparison between males and females in LTHW	45
4.24	comparison between males and females in LTBW	46
4.25	comparison between males and females in LTTW	46

List of tables:

No	Table title	Page
1	2.1demonstrates developmental classification	6
2	: 4.1: Characteristics of subjects enrolled in Magnetic Resonance Imaging studies of the Caudate Nucleus	33
3	4.2:: Characteristics of subjects enrolled in Magnetic Resonance Imaging studies of the caudate nucleus according to age group:	33
4	4.3:comparison between males and females	40

List of abbreviations:

MRI	Magnetic Resonance Imaging
NMR	nucleur magnetic resonance imaging
MHz	mega hertz
SNC	substantianigra pars compacta
SNr	substantianigra pars reticulate
STN	Subthalamic
AD	Alzheimer disease
APP	amyloid precursor
HD	Huntington disease
CAG	cytosine adenine guanine
T	Tesla
FMRI	functional Magnetic Resonance Imaging
RTHL	right head length
RTBL	right body length
RTTL	right tail length
RTHW	right head width
RTBW	right body width
RTTW	right tail width
RTHL	right head length
RTBL	right body length
RTTL	right tail length
RTHW	right head width
RTBW	right body width
RTTW	right tail width

Chapter one

INTRODUCTION

Chapter one

1.1 Introduction

The caudate nucleus considers important structure because it has important functions in control of movement and planning and execution.

These functions normally change with aging and age –related changes of caudate nucleus increases prevalence neurodegenerative diseases including ; Parkinson’s and Huntington’s disease

These changes have laded to increase need to knowing pattern of age – related atrophy of brain tissue and to understand the normal aging of brain and also to identify causes and possible role of disease in decreasing brain function with age

Therefore morphometry and analysis of caudate nucleus in normal population essential to monitor clinical outcomes of neurodegenerative diseases.

To study caudate nucleus there are two methods ; postmortem and imaging

The postmortem doesn’t provide realistic results and has several limitations such as fixation artifact and volume shrinkage so isn’t reliable method for volumetric studies

The second method is imaging such as using MRI it has better tissue contrast and non-invasive MRI imaging increases the accuracy of the morphometric measurement

Because of the lack of studies for caudate nucleus measurements to determine the average range of caudate nucleus dimensions in Sudanese population

1.3 General Objective:

Measurement of normal caudate nucleus dimensions in magnetic resonance images for Sudanese population

1.3.1 Specific objectives:

- To measure the length of the caudate nucleus
- To measure the width of the caudate nucleus
- To compare between size of caudate nucleus in relation to age

To compare between male and female caudate nucleus measurements

1.4 Significance of the study

This study will provide a Sudanese index (dimension) for caudate nucleus in Sudanese and the changes in the measurement that attributed to age. As well as the textural identity for the caudate nucleus as normal structures which will facilitate the identification of the pathological condition, which might be subtle in the normal visual perception evaluation.

Chapter two

Literature review and previous studies

Chapter two

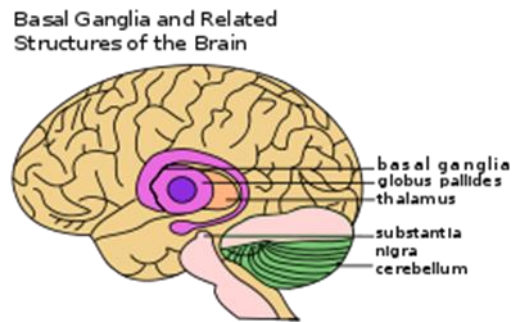
Background

2.1 Anatomy

The basal ganglia form a major brain system in all species of vertebrates, but the basal ganglia of primates (including humans) have special features that justify a separate consideration. As in other vertebrates, the primate basal ganglia can be divided into striatal, pallidal, nigral, and subthalamic components. In primates, however, the two pallidal subdivisions are called the external and internal (or sometimes lateral and medial) segments of the globus pallidus, whereas in other species they are called the globus pallidus and entopeduncular nucleus. (www.en.wikipedia.org.)

Also in primates, the striatum is divided by a large tract of white matter called the internal capsule into two masses of gray matter that early anatomists named the caudate nucleus and putamen in most other species no such division exists, and only the striatum as a whole is recognized. Beyond this, the complex topography of connections between the striatum and warranted by the fact that different types of information are cortex means that functions are segregated within the primate striatum in ways that do not apply to other species. (www.en.wikipedia.org)

A separate consideration of the primate basal ganglia is also available than for other species. Large areas of the primate brain are devoted to vision; consequently the role of the basal ganglia in controlling eye movements has been studied almost exclusively in primates. Functional imaging studies have been performed mainly using human subjects. Also, several major degenerative diseases of the basal ganglia, including Parkinson's disease and Huntington's disease, are specific to humans, although "models" of them have been proposed for other species



Basal ganglia

www.en.wikipedia.org/basal.ganglia

2.1.1 Anatomical subdivision and connection:-

In terms of development, the human nervous system is often classified based on the original 3 primitive vesicles from which it develops: These primary vesicles form in the normal development of the neural tube of the human fetus and initially include prosencephalon, mesencephalon, and rhombencephalon, in rostral to caudal (from head to tail) orientation. Later in development of the nervous system each section itself turns into smaller components. During development, the cells that migrate tangentially to form the basal ganglia are directed by the lateral and medial ganglionic eminences (www.en.wikipedia.org)

Table 2.1 demonstrates the developmental classification and traces it to the anatomic structures found in the basal ganglia

Primary division of the neural tube	Secondary subdivision	Final segments in a human adult
prosencephalon	1.telencephalon 2.diencephalon	1.On each side of the brain: the cerebral cortices, caudate, putamen 2.Globus Pallidus(pallidum), Thalamus, hypothalamus, subthalamus, epithalamus, subthalamic nuclei
mesencephalon	1.mesencephalon	1.Mesencephalon (midbrain): substantianigra pars compacta (SNc), substantianigra pars reticulata (SNr)
Rhombencephalon	1.metencephalon 2.myelencephalon	1.Pons and cerebellum 2.Medulla

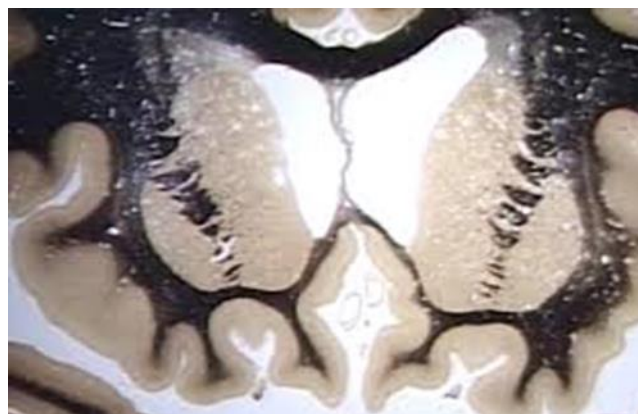


Figure 2. 2 Coronal slices show head of caudate nucleus

<http://peir.path.uab.edu/library/picture.php?/31589>

The basal ganglia form a fundamental component of the cerebrum. In contrast to the cortical layer that lines the surface of the forebrain, the basal ganglia are a collection of distinct masses of gray matter lying deep in the brain not far from the junction of the thalamus. Like most parts of the brain, the basal ganglia consist of left and right sides that are virtual mirror images of each other.

In terms of anatomy, the basal ganglia are divided by anatomists into four distinct structures, depending on how superior or rostral they are (in other words depending on how close to the top of the head they are): Two of them, the striatum and the pallidum, are relatively large; the other two, the substantianigra and the subthalamic nucleus, are smaller. In the illustration to the right, two coronal sections of the human brain show the location of the basal ganglia components. Of note, and not seen in this section, the subthalamic nucleus and substantianigra lie farther back (posteriorly) in the brain than the striatum and pallidum (www.en.wikipedia.org)

Striatum:-

The striatum is the largest component of the basal ganglia. The term "striatum" comes from the observation that this structure has a striped appearance when sliced in certain directions, arising from numerous large and small bundles of nerve fibers (white matter) that traverse it. Early anatomists, examining the human brain, perceived the striatum as two distinct masses of gray matter separated by a large tract of white matter called the internal capsule. They named these two masses the "caudate nucleus" and "putamen".

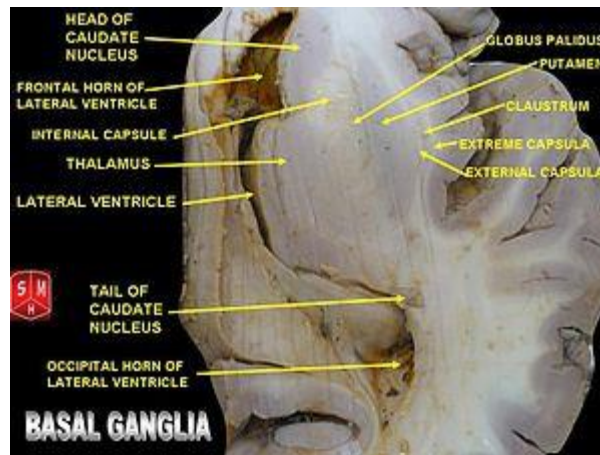


Figure 2.3.basal ganglia

www.en.wikipedia.org/basal.ganglia

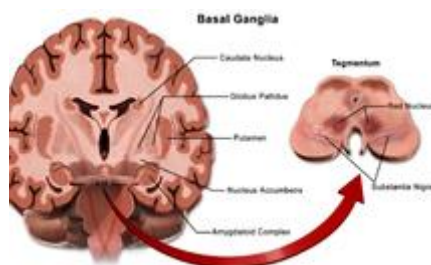
Pallidum:-

The *pallidum* consists of a large structure called the globuspallidus ("pale globe") together with a smaller ventral extension called the ventral pallidum. The globuspallidus appears as a single neural mass, but can be divided into two functionally distinct parts, called the internal (or medial) and external (lateral) segments

Substantianigra:-

The substantianigra is a mesencephalic gray matter portion of the basal ganglia that is divided into SNr (reticulata) and SNc (compacta). SNr often works in unison with GPi, and the SNr-GPi complex inhibits the thalamus

(www.en.wikipedia.org)



www.en.wikipedia.org/ location of basal ganglia

Subthalamic nucleus:-

The subthalamic nucleus (STN) is a diencephalic gray matter portion of the basal ganglia, and the only portion of the ganglia that produces an excitatory neurotransmitter,

(basal ganglia-wikipedia)

2.2 Physiology:-

Neurochemistry

The caudate is highly innervated by dopamine neurons that originate from the substantianigra pars compacta (SNc). The SNc is located in the midbrain and contains cell projections to the caudate and putamen, utilizing the neurotransmitter dopamine. There are also additional inputs from various association cortice

(www.en.wikipedia.org)

Spatial Mnemonic Processing

The caudate nucleus integrates spatial information with motor behavior formulation. Selective impairment of spatial working memory in subjects with Parkinson's disease and the knowledge of the disease's impact on the amount of dopamine supplied to the striatum have linked the caudate nucleus to spatial and nonspatial mnemonic processing. Spatially dependent motor preparation has been linked to the caudate nucleus through event-related fMRI analysis techniques

(www.en.wikipedia.org)

Directed Movements

The caudate nucleus contributes importantly to body and limbs posture and the speed and accuracy of directed movements. Deficits in posture and accuracy during paw usage tasks were observed following the removal of

caudate nuclei in felines. A delay in initiating performance and the need to constantly shift body position were both observed in cats following partial removal of the nuclei.

Memory

The dorsal-prefrontal cortex subcortical loop involving the caudate nucleus has been linked to deficits in working memory, specifically in schizophrenic patients. Functional imaging has shown activation of this subcortical loop during working memory tasks in primates and healthy human subjects. The caudate may be affiliated with deficits involving working memory from before illness onset as well. Caudate nucleus volume has been found to be inversely associated with perseverative errors on spatial working memory tasks.

(www.en.wikipedia.org)

Emotion

The caudate nucleus has been implicated in responses to visual beauty, and has been suggested as one of the "neural correlates of romantic love

Language

The left caudate in particular has been suggested to have a relationship with the thalamus that governs the comprehension and articulation of words as they are switched between languages.

(www.en.wikipedia.org)

Threshold control

The brain contains large collections of neurons reciprocally connected by excitatory synapses, thus forming large network of elements with positive feedback. It is difficult to see how such a system can operate without some mechanism to prevent explosive activation. There is some indirect evidence that the caudate may perform this regulatory role by measuring the general activity of cerebral cortex and controlling the threshold potential.

(www.en.wikipedia.org)

2.3 Pathology:-

2.3.1 Alzheimer disease (AD)

the most common cause of dementia in the elderly, with cerebrovascular disease and several less common neurodegenerative disorders accounting for most of the remaining cases. Most cases of AD occur after the age of 50, with a progressive increase in incidence with increasing age. Most cases are sporadic, but in roughly 10% of patients, there is a family history of dementia. As will be discussed, these familial cases have provided important insights into the pathogenesis of AD. Morphologic changes identical to those seen in AD are also almost invariably present in patients with Down syndrome who survive beyond the age of 40. Although the cause of AD remains unknown, a number of factors have now been identified that appear to play a major role in the development of this disorder

- Genetic factors play a role in the development of some cases of AD, as evidenced by the occurrence of familial cases. Studies of familial cases have provided significant insights into the pathogenesis of familial, and possibly sporadic, AD. Mutations in at least four genetic loci have been linked conclusively to familial AD. In view of the long-recognized association between trisomy 21 and AD-like changes in the brain, it is perhaps not surprising that the first of these to be identified was a locus on chromosome 21, now known to encode a protein known as amyloid precursor protein (APP)
- Deposition of a form of amyloid, derived from breakdown of APP, is a consistent feature of AD. The breakdown product, known as β -amyloid ($A\beta$), is a prominent component of the senile plaques found in the brains of AD patients
- Hyperphosphorylation of the protein tau represents yet another piece of the AD puzzle. Tau is an intracellular protein that is involved in the assembly of intra-axonal microtubules. In addition to amyloid deposition, cytoskeletal abnormalities are an invariant feature of AD. Many of these structural abnormalities are associated with accumulation of hyperphosphorylated forms of tau, the presence of which may interfere with maintenance of normal

microtubules. While invariably present in AD, tau-associated cytoskeletal abnormalities are not restricted to that disorder; they are encountered in a variety of other neurodegenerative disorders and conditions as diverse as metabolic diseases (Niemann-Pick disease), neoplasms (gangliogliomas), and hamartomas. Whether hyperphosphorylation of tau protein represents a primary event in the pathogenesis of AD, or a secondary event, remains to be established. Until very recently, there appeared to be no linkage between the formation of abnormal tau proteins and amyloid deposition. Now the proponents of the tau hypothesis ("tauists") and the β -amyloid hypothesis (" β taptists") may have found a point of convergence. It appears, at least in murine models of Alzheimer disease, that APP or its product A β amyloid increases the formation of neurofibrillary tangles derived from tau proteins.

2.3.2 Parkinsonism

Parkinsonism is a disturbance in motor functions characterized by rigidity, expressionless facies, stooped posture, gait disturbances, slowing of voluntary movements, and a characteristic "pill-rolling" tremor. Parkinsonism is not a single disease but rather is the clinical manifestation of a disturbance in the dopaminergic pathways connecting the substantianigra to the basal ganglia. Such disturbances occur in a number of other degenerative diseases and may also be caused by trauma, certain toxic agents (notably a compound known as MPTP, a contaminant found in some batches of illicitly manufactured meperidine), vascular diseases, and encephalitis.

Perhaps the best known form of parkinsonism is that associated with Parkinson disease, also known as idiopathic parkinsonism or paralysis agitans. Parkinson disease is a degenerative disorder involving the dopamine-secreting neurons of the substantianigra, as well as the locus ceruleus. It is a disease of adulthood, with most cases becoming manifest by the sixth decade. Although most cases arise sporadically, it is likely that genetic factors play a role in the development of the disease in some of these patients, perhaps by increasing susceptibility to an environmental toxin. Genetic abnormalities play a more obvious role in the uncommon familial cases of Parkinson disease. Mutations in a gene coding for a protein involved in

normal neuronal synapses, termed α -synuclein, account for at least some of these familial cases.

{Robbins basic pathology 7th edition}

2.3.3 Huntington disease (HD)

is a hereditary, progressive, fatal disorder involving the "extrapyramidal" motor system, characterized by involuntary movements (chorea) and dementia. The disease is inherited as an autosomal dominant trait with complete penetrance. It usually does not become apparent until adulthood, often after affected individuals have had children, although juvenile-onset cases also occur. Early-onset cases, in particular, are more likely to be associated with inheritance of the mutation from the father than from the mother. The responsible gene (which encodes a protein called huntingtin) has been localized to the short arm of chromosome 4. The disease is caused by trinucleotide repeat mutations in the huntingtin gene), which cause, in turn, the synthesis of a form of the huntingtin protein containing an abnormal number of glutamine residues. The normal huntingtin gene contains between 6 and 34 copies of the cytosine-adenine-guanine (CAG) sequence. In HD, the number of triplet repeats is increased, with most HD patients carrying between 40 and 55 CAG copies. The larger the number of trinucleotide repeats, the earlier the onset of disease; patients with juvenile-onset HD, for example, typically carry greater than 70 CAG repeats. Affected individuals can be identified before the development of symptoms by the demonstration of excessive CAG triplet repeats in the responsible gene. The identification of individuals in the presymptomatic phase of their disease obviously carries with it an immense ethical burden and should not be undertaken in the absence of appropriate counseling.

The molecular pathogenesis of HD is not fully understood. Huntingtin is expressed in all somatic tissues, and its expression is clearly essential to normal embryonic development. Nevertheless, the exact function of huntingtin remains unknown. Because HD is an autosomal dominant disorder, it follows that the mutant huntingtin in some manner impairs the function of normal huntingtin produced by the normal allele. Such mutations are referred to as

"gain of function" mutations. Although the exact mechanism whereby the mutant huntingtin causes brain injury remains unclear, it is likely that the presence of abnormal huntingtin causes cell loss by some combination of activation of apoptotic pathways and impairment of normal energy metabolism in susceptible neurons.

{Robbins basic pathology 7th edition}

2.3.4 Schizophrenia

Schizophrenia is a frightening illness in which intrusive "voices" (auditory hallucinations) frequently torment the individual with abusive or derogatory comments, and ideas weave together to form false

beliefs (delusions). The sufferer may be convinced he is under surveillance or enmeshed in a conspiracy of huge religious or political significance

He may believe that his thoughts are no longer private or that they are controlled by an external, and usually malevolent, will.

The onset of psychosis may be characterised by *delusional mood* consisting of intense puzzlement, with familiar surroundings seeming strange, relationships seeming changed and a feeling that something inexplicable or sinister is going on. Patients may also suffer perceptual abnormalities such as faces changing shape or experience odd smells or tastes (e.g. of blood or poison). In addition to auditory hallucinations, some patients have somatic hallucinations (e.g. of a sexual nature) or, less commonly, visual hallucinations.

Delusions are most frequently of a paranoid nature but may also be religious, grandiose or sexual.

Most people recover from their first schizophrenic episode within a few weeks of receiving antipsychotic drugs, but with each succeeding episode, the hallucinations and delusions (termed *positive symptoms*) may become more resistant to treatment.

Nayani and David (1995) have shown how the psychotic experiences appear to gradually "colonise

the healthy parts of the mind. In particular, they describe how delusional explanations gradually become more complex and bizarre. In this way, one patient interpreted the ordinary anxiety-related experience of tightness of the throat as “a penis being forced down my throat and suffocating me”.

Thought disorder. Patients may show derailment of thought or the so-called knight’s-move thinking, and illogical speech may deteriorate to the point that it becomes incoherent. There may be dislocation of words or, occasionally, the creation of new private words (neologisms), sometimes by the condensation of others; for example, a patient whose initials were K.A.O. described his personal philosophy as “Kaosophy”. Individuals with schizophrenia may also give private idiosyncratic meanings to words that already exist

(*Essential Psychiatry*, ed. Robin M. Murray)

2.4 MRI machine

2.4.1 Basic Principle of MRI

Magnetic resonance imaging (MRI) is founded on the principle of nuclear magnetic resonance (NMR). The principles of nuclear magnetic resonance are based on the fact that the nuclei of certain elements have a magnetic moment. This means that if a sample of atoms of one of these elements were placed in a magnetic field, its nuclei would tend to line up with the field.

The nuclei don't actually line up exactly in the direction of the magnetic field, however. The laws of quantum mechanics dictate that they align at an angle to the direction of the field.

Each type of nucleus has a quality known as angular momentum associated with it. The idea of an intrinsic angular momentum of the nucleus is fundamental to magnetic resonance imaging. It can be likened to the example of a spinning top. When a top is spun at an angle to the vertical, it will precess about the vertical axis. That is, the top will rotate about its own axis, and the axis of the top's rotation will revolve about the vertical axis.

This precession is due to the angular momentum of the top, which is in turn due to the spinning of the top, in the same way; a nucleus that is aligned at an angle to the direction of the magnetic field will precess about the axis of the field.

The analogy is so exact that the nuclei are commonly referred to as spins that are manipulated to generate images.

In quantum mechanics a number called the spin of the nucleus represents the angular momentum. Depending on the value of the spin number of a particular, there will be several different orientations in which the nuclei may line up in a magnetic field. Each orientation is represented by a different angle from the direction of the magnetic field about which the nucleus will precess.

MRI takes advantage of the fact that the nucleus of a hydrogen atom (a single proton) has a magnetic moment. The spin of the proton is such that the proton has exactly two possible ways to line up with the applied magnetic field. Because of its abundance in the body, hydrogen is a wonderful candidate for use in magnetic resonance imaging.

The frequency at which the nucleus precesses is a function of both the strength of the magnetic field and the particular nucleus. This frequency, called the Larmor frequency, and is equal to the product of the strength of the magnetic field and a constant called the gyro-magnetic ratio. The gyro-magnetic ratio is unique for each nucleus that has a magnetic moment (Catherine Westbrook, 2008).

The Larmor frequency is important, because it's the frequency at which the nucleus will absorb energy that will cause it to change its alignment. In proton imaging this energy is in the radio frequency (RF) range, meaning that the frequency typically varies from (1 to 100) MHz. If an RF pulse at the Larmor frequency B_0 is applied to a proton, the proton will change its alignment so that rather than being aligned with the main magnetic field, it will be aligned opposite the field. Over a period of time the proton will flip back to align with the field. In doing so, it will emit energy whose frequency is also exactly the

larmor frequency. It is this emission of energy that made NMR such a useful means to locate on image protons(Catherine Westbrook, 2008).

The term resonance refers to that property of the procession nucleus in which it absorbs energy only at the larmor frequency. If the frequency is off even by a small amount, the nucleus will not absorb any energy, nor will it change state. (Catherine Westbrook, 2008)

2.4.2MRI Instrumentation:

The MRI system consists of, the magnet, the gradient coils, the radiofrequency subsystem and the computer. (Catherine, 2008)

2.4.2.1 The Magnet:

The heart of all MR system is the magnet. There are three types of the magnets in common use for MRI; all have in common that they can generate large uniform magnetic fields. They differ in the cost to produce the magnet, the strength that can be produced, energy requirement to support the magnet, and the direction of the main magnetic fields. (Catherine, 2008)

2.4.2.2 Super Conducting Magnets: -

By far the most commonly used magnet is the superconducting magnet. This type of magnet is notable in that the magnetic field can be maintained for a very long period of time without requiring a constant source of energy. This allows the use of this type of magnet in systems that require extremely strong magnetic field (above 0.5 T). (Catherine, 2008)

A superconducting magnet consists of many winding of wire that carries on electric current. The magnet field generates by this cylinder of wires runs in the direction along the long axis of the cylinder. When used to produces MR. Images the superconducting magnet produces relatively high magnetic field strength with low power requirement. (Catherine, 2008)

2.4.2.3 Resistive Magnets: -

Resistive magnets are similar to superconducting magnets, in that they are typically coils of wire through which a magnetic field is induced. However, the wires aren't cooled to a superconductive state. Therefore, the wires are resistive, and if a current were applied and the power supply disconnected the current would eventually die out.

The major difference, therefore, is one of tradeoffs in operating cost. A resistive magnet doesn't require liquefied gases (cryogenics), but it does require a power supply to keep the magnet at a stable field. As a result of the increase in cost, these magnets aren't seen in commercial systems at field strengths over 0.4 T. (Catherine, 2008)

2.4.2.4 Permanent Magnets

The permanent magnet is gaining in popularity for systems that operate at magnetic fields up to about 0.4T. A large part of this popularity is due to the fact that a permanent magnet has few requirements to maintain it. While a superconducting magnet requires cryogenics, and a resistive magnet requires a power supply to maintain its current a permanent magnet requires neither.

The disadvantages of using a permanent magnet are its weight and the cost of the magnet and supporting structure. In addition, permanent magnets are susceptible to hysteresis (a time varying change in the field). They are commonly used now for low cost systems; the cost (and weight) of the magnets has precluded their use at higher field strengths. (Catherine, 2008)

2.4.3 Types of Coils according to the usage:

2.4.3.1 Shim Coils:

Due to design limitations it's almost impossible to create an electromagnet, which produces a perfectly homogeneous magnetic field. To correct for these inhomogeneities, other loops of current carrying wire are placed around the bore. This process is called shimming and the extra loop of wire is called a shim coil. Shim coils produce magnetic field evenness or homogeneity. For

imaging purposes, homogeneity of the order of 10 ppm is required. Spectroscopic procedures require a more homogeneous environment of 1 ppm.

The shim system requires a power supply which is separate from the other power supplies within the system. This is important because a fault in the shim power supply compromises image quality. (Catherine, 2008)

2.4.3.2 Gradient Coils:

The magnetic field strength is proportional to the amount of current passed through the loop of wire, the number of loops in the wire, the size of the loops, and how closely the loops are spaced. If the loops are spaced closely at one end of the solenoid and gradually become farther apart at the other end, the resultant magnetic field becomes stronger at one end than the other. This is called a magnetic field gradient. Gradient coils provide a linear gradation or slope of the magnet field strength from one end of the solenoid to the other. The gradient is applied by passing current through the gradient coils in a certain direction. The amplitude of the gradient slope is determined by the magnitude of the current passing through the coil. (Catherine, 2008)

By varying the magnetic field strength, gradient provide position dependent variation of signal frequency and are therefore used for slice selection, frequency encoding, phase encoding, rewinding and spoiling. Gradient coils are powered by gradient amplifiers. Faults in the gradient coils or gradient amplifiers can result in geometric distortion in the MR image. (Catherine, 2008)

2.4.3.3 Radio Frequency Coils:

The energy required to produce resonance of nuclear spins is expressed as a frequency and can be calculated by the Larmor equation. At field strengths used in MRI, energy within the radio frequency (RF) band of the electromagnetic spectrum is necessary to perturb or excite the spins. As shown by the Larmor equation, the magnetic field strength is proportional to the RF, the energy of which is significantly lower than that of X-rays. In order

to produce an image, RF must first be transmitted at the resonant frequency of hydrogen so that resonance can occur. The transverse component of magnetization created by resonance must be detected by a receiver coil. (Catherine, 2008)

The configuration of the RF transmitter and receiver probes or coil directly affects the quality of the MR signal. There are several types of coils currently used in MR imaging. These are:

2.4.3.4 Volume Coils

A volume coil both transmit RF and receives the MR signal and is often called a transceiver. It encompasses the entire anatomy and can be used for either head or total body imaging. Because of their large size they generally produce images with lower SNR than other types of coils. (Catherine, 2008)

2.4.3.5 Surface Coils :

Coils of this type are used to improve the SNR when imaging structures near the surface of the patient (Such as lumbar spine). As the SNR is enhanced when using local coils (surface coils) greater spatial resolution of small structures can often be achieved when using local coils, the body coil is used to transmit RF and the local coil is used to receive the MR signal. (Catherine, 2008)

2.4.3.6 Phase Array Coils:

Phased array coils are now widely used. These consist of multiple coils and receivers whose individual signals are combined to create one image with improved SNR and increased coverage. Therefore the advantages of small surface coil (increased SNR and resolution); can be combined with a large FOV for increased anatomy coverage. Usually up to four coils and receiver are grouped together to increase either longitudinal coverage (for spin imaging), or to improve uniformity across a whole volume (pelvic imaging). (Catherine, 2008)

2.4.3.7 Circumferential Coils:

At the point where depth equals radius of the structure being imaged, the coil may be placed around the object in a circumferential fashion to form a solenoid. Circumferential coils provide good signal responses across the image because all points are within one radius from the edge of the coil. Two general configurations are possible with circumferential coils: solenoidal and saddle. It can be used to image the neck, knee, ankle and pediatric. (Catherine, 2008)

2.4.4 The computer system

MRI computer systems vary with manufacture. Most however consist of:

Aminic computer with expansion capabilities, An array processor for Fourier transformation. An image processor that takes data from the array processor to form an image. Hard disc drives for storage of raw data and pulse sequence parameters. A power distribution mechanism to distribute and filter the alternating current. (Catherine, 2008)

2.4.5 Conventional spin echo:

The spin echo sequence utilizes a 90° excitation pulse to flip the net magnetization vector (NMV) into the Transverse plane. The NMV precesses in the transverse plane, inducing a voltage in the receiver coil. The precession paths of the magnetic moment of the nuclei within the NMV are translated into the transverse plane. When the 90° RF pulse is removed a free induction decay signal (FID) is produced. T2 dephasing occurs immediately and the signal decays. A 180° RF pulse is then used to compensate for this dephasing.

Spin echo pulse sequences are the gold standard for most imaging. They may be used for almost every examination. T1 weighted images are useful for demonstrating anatomy because they have a high signal to noise ratio (SNR). In conjunction with contrast enhancement however, they can show pathology. T2 weighted also demonstrate pathology. Tissues that are diseased are generally more edematous and/or vascular. They have increased water

content and consequently, have high on T2 weighted image and can therefore be easily identified. The conventional spin echo has the advantages of good image quality, very versatile and true T2 weighted sensitive to pathology. They have the disadvantages of requiring longer scan time. (Catherine, 2008)

2.4.6 Fast Spin Echo (Turbo Spin Echo):

As the name suggests, fast spin echo (FSE) is a spin echo pulse sequence, but with scan times that are drastically shorter than conventional spin echo.

As the scan time is a function of the TR, NEX and number of phase encoding, in order to reduce the scan time, one or more of these factors should be reduced. Decreasing the TR and the NEX affects image weighting and SNR which is undesirable. Reducing the number of phase encodings reduces the spatial resolution, which is also a disadvantage. In fast spin echo, performing more than one phase encoding step and subsequently filling more than one line of K space per IR reduce the scan time. This is achieved by using an echo train that consists of several 180°-rephrasing pulses, at each rephrasing an echo is produced and a different phase encoding step is performed. (Catherine, 2008)

In conventional spin echo, raw image from each echo stored in K space, and the numbers of 180° rephrasing pulses applied corresponds to the number of echoes produced per TR. Each echo is used to produce a separate image. In fast spin echo, data from each echo is placed into one image. The number of 180° rephrasing pulses performed per TR corresponds to the number is called the turbo factor or the echo train length. As the turbo factor increase, the scan time decrease, as more phases encoding steps are performed per TR. (Catherine, 2008)

The advantages of the fast spin echo is that, the scan times greatly reduced, high-resolution matrices and multiple NEX can be used, and image quality improved, and increased T2 information.

The disadvantages are some flow and motion affects increased, incompatible with some imaging options, fat bright on T2 weighted images, image blurring

can result as data is collected at different TE times, reduce magnetic susceptibility effect as multiple 180° pulses produce excellent rephasing so it should not be used when haemorrhage is suspected

In recent years, fast spin echo (FSE) sequences have begun to replace conventional spin echo sequences. (Catherine, 2008)

2.4.7 The Gradient Echo Pulse Sequence:

A gradient echo pulse sequences utilizes an RF excitation pulses that is variable, and therefore flips the NMV through any angle (not just 90°). A transverse component of magnetization is created, the magnitude of which is less than in spin echo, where all the longitudinal magnetization is converted to the transverse plane. When a flip angle other than 90° is used only part of the longitudinal magnetization is converted to transverse magnetization, Gradient echo pulse sequences can be acquired T2*, T1 and proton density weighted, however, there is always some degree of T2* weighted present on any image due to the absence of 180° rephrasing pulse. Gradient echo sequence allow for reduction in the scan time as the TR is greatly reduced. They can be used for signal slice breath-hold acquisition in the abdomen, and for dynamic contrast enhancement. They are very sensitive to flow a gradient rephrasing is not slice selective, so flowing nuclei always give a signal, as long as they have been previously excited. Because of this, gradient echo sequences may be used to produce angiography, type images.

They provide interesting capabilities in term of contrast and speed. These techniques can be broadly divided into " steady state " sequences, such as gradient recalled steady state (GRASS) and fast imaging with steady state free precession (FISP), and " spoiled " sequences, such as fast low-angle signal-shot (FLASH) and (spoiled GRASS). (Catherine, 2008)

2.4.8 Three-Dimensional Fourier Transform (3DFT):

The great attraction of this technique is that a high resolution volume data set can be processed retrospectively to generate any arbitrarily oriented plane of section. For instance, a radial image can be produced using suitable

software. Three-dimensional acquisition is only practical with fast scan sequences.

The advantages of 3DFT imaging are the ability to acquire thin section without gaps and the potential for 3D rendering and reformatting. The disadvantages of 3DFT imaging is that the costs include a significantly larger requirement for resources such as computing power, memory, display, and storage. Other less well-established concerns are that the examinations may take longer to interpret, given that more sections must be viewed, and that there may be a penalty in signal-to-noise and contrast, which accompanies the requirement. (Catherine, 2008)

2.4.9 Inversion Recovery:

Inversion recovery is a pulse sequences that begins with a 180° inverting pulse. This inverts the net magnetization vector (NMV) through 180° into full saturation. When the inverting pulse is removed the NMV begins to relax back to B_0 .

A 90° excitation pulse is then applied at a time from the 180° inverting pulse know as time from inversion (I_1). The contrast of the resultant image depends primarily on the length of the T_1 . If the 90° excitation pulse is applied after the NMV has relax back through the transverse plane the contrast in the image depend on, the amount of longitudinal recovery of each vector (as in spin echo). The resultant image is heavily T_1 weighted, as the 180° inverting pulse achieves full saturation and ensure a large contrast difference between fat and water.

If the 90° excitation pulse is not applied until the NMV has reached full recovery, a proton density image result, as both fat and water have full relaxed.

After the 90° excitation pulse, a 180° rephasing pulse is applied at a time T_B after excitation pulse. This produces a spin echo. The T_R is the time between each 180° inverting pulse.

Inversion recovery is used to produce heavily T₁ weighted images to demonstrate anatomy. The 180° inverting pulse produce a large contrast difference between fat and water because full saturation of the fat and water vectors is achieved at the beginning of each repetition. Inversion recovery pulse sequences therefore produce more heavy T₁ weighting than conventional spin echo and should be used when this is required. As the use of contrast primary shortens T₁ times of certain tissue, IR pulse sequences increase the signal from structures that have enhanced as a result of a contrast injection.

Inversion recovery has the advantages that it gives very good SNR, as the TR is long and excellent T₁ contrast. The disadvantage that is it spends along scan times unless used in conjunction with fast spin echo. (Catherine, 2008)

2.4.10 STIR (short T₁ inversion recovery):

Is an inversion recovery pulse sequence that uses a T₁ that corresponds to the time it takes fat to recover from full inversion to the transverse plane so that there is no longitudinal magnetization corresponding to fat, When the 90° excitation pulse is applied, the fat vector is flipped through 90° to 180° and into full saturation, so that the signal from fat is nulled. STIR is used to achieve suppression of the fat signal in a T₁ weighted image.

One of the advantages of STIR is that it is relatively reliable and system independent. As in spin echo, the contrast mechanism can be fairly easily reproduced from system to system and field strength to field strength, with appropriate correction of timing parameters. (Catherine, 2008)

The primary disadvantages lies with scan time. STIR scan time, as for inversion recovery sequences, can be computed as the product {TR x NEXx Matrix}. Since relatively long TR values are generally used, this resultant in scans times comparable to even longer than standard T₂ weighted spin echo sequences. (Catherine, 2008)

In addition, we must be careful in the use contrast agent in conjunction with STIR sequences. Gadolinium will shorten the T₁ relaxation rate for

vascularity, its T1 value will not be affected, and however, fatty lesions may experience some T1 shortening and therefore have reduced effectiveness in fat suppression. The combination of STIR with gadolinium enhancement has proven useful in the evaluation of breast lesion where sufficiently suppression of the fat signal combined with enhancement of the lesion has been shown to increase detectability. (Catherine, 2008)

2.4.11 Spectral pre-saturation Inversion Recovery (SPIR):

This method is a combination of the spectral saturation and (STIR) routines it is available on Philips scanners where it is designated Spectral Inversion Recovery (SPIR and GE scanners with the designation Spectral Inversion at Lipids (SPECIAL). The idea is to apply a spectrally selective pulse to flip fat spins then, after the time interval that lets the Mz of fat reach zero, the excitation pulse is applied and the signal of the water spins give most of the signal.

Time is the major disadvantage of this fat suppression method. The routine is best applied at least once per TR, and for multi-slice sequences once per slice per TR. The best fat suppression is achieved with a 180 degree spectral inversion pulse and a time delay equal that used in normal STIR imaging (approximately 150 msec at 1.5 T) plus the finite time required for the inversion pulse) This is clearly impractical for anything but extremely long TR techniques.

In practice the "inversion" pulse used ranges between slightly more than 90 degrees but significantly less than 180 degrees the required delay time can be acceptably short. In most scanners using this method the radiographer has control of the inversion flip angle and the system determines the optimum delay time The routine is applied in a "segmented" fashion allowing some small variation in the degree of fat suppression across slices.

SP1R will be as sensitive to local field inhomogeneity as spectral saturation routines. It is suitable for use after Gd contrast because only the fat spins are affected by the routine. (Catherine, 2008)

2.5 Previous studies

- **Am J psychiatry, 2002 jul:159(7):1190-1191** First, the authors found significantly lower left and right absolute (13.1%, 13.2%) and relative (9.1%, 9.2%) caudate nucleus volumes in never-medicated subjects with schizotypal personality disorder than in normal subjects. Second, they found significant, inverse correlations between caudate nucleus volume and the severity of perseveration in two distinct working memory tasks in these neuroleptic-naive subjects with schizotypal personality disorder
- **Pol J Radiol 2013 Jul-Sep; 78(3): 7–14** Bilateral age-related shrinkage and rightward asymmetry of the striate nucleus was found in healthy adults and there were significant volume differences between men and women. Obtained results provide useful baseline data on age and gender-related changes of the volume of the striatum.
- **Journal of Paramedical Sciences (JPS)** Spring 2013 Vol.4, No.2 ISSN 2008-4978
- The results of the statistical analysis on age related changes for both sides of the caudate and putamen volumes . There exist significant negative correlations between age and caudate volume in male group (right side: $r=-0.718$, $P<0.001$; left side: $r=0.721$, $P<0.001$). In female group, there exist significant negative correlations between age and caudate volume (right side: $r=-0.627$, $P<0.001$; left side: $r=-0.569$, $P<0.001$). In male group, the negative association between age and the volumes of caudate nucleus were stronger than female group ($P< 0.01$). However, there were significant differences between age groups in the volumes of caudate. Men in the young group had significantly larger total volumes for the caudate nucleus than the old group (8.92 vs 7.12cm³ respectively, $P<0.001$) .In comparison to old group, men in the young group had larger measured volumes of right (4.55 vs 3.63cm³ respectively, $P<0.001$) and left (4.37 vs 3.49cm³ respectively, $P<0.001$) caudate nucleus. In women between two age groups, the young group had significantly larger total measured volumes for caudate (8.42 vs 6.79cm³

respectively, $P < 0.001$). Besides, measured volumes of right caudate (4.34 vs 3.47 cm³ respectively, $P < 0.001$), left caudate (4.09 vs 3.32 cm³ respectively, $P < 0.001$) was larger in the young group. Effect of sex on striatum volume The descriptive statistics for the volume of the right or left caudate nucleus by age \times sex \times group are presented in Table 1. The older men had larger right (3.63 vs 3.47 cm³ respectively, $P = 0.63$) and left (3.49 vs 3.32 cm³ respectively, $P = 0.55$) caudate volumes than the older women. Across the two age groups, there were no statistically significant volume differences between the two sexes for the right and left caudate nucleus ($P > 0.05$). Furthermore, the rate of reduction of the striatum volume (age \times sex) was used to assess the degree of volume shrinkage with a span between 15 and 65 years old. For this region, there was a significant age-related decrease in the volumes of caudate for men and women. The observed volume reduction rate by age and sex for men were 4.9% and 4.5% and for women were 3.3% and 2.9% for the right and left caudate, respectively (Fig. 2, 3). Overall rate of decrease was less for women than men and interaction of gender with age was significant (for caudate $P = 0.036$ and for putamen $P = 0.008$) suggesting that the rates of caudate and putamen volume decrease with age are different between two sexes

- Direct linear measurement of caudate nucleus widths are more accurate than indirect measurement (bi-caudate distance) in detecting early atrophic changes using MRI in patients with Huntington's disease (IID) At 95% confidence level caudate nucleus widths of 8mm or less were found to be abnormal . While those 9mm or larger were normal.

Caudate nucleus width were more sensitive than similar measurement of the putamen or of bi-caudate skull ratios as correlates of function changes patients with early HD (DanidK.Kidoil.Shoulson,J.VMsnziona,P.P. Harnish)

- Caudate nucleus atrophy occurs in Huntington's disease and methods of measuring this have been described using axial CT but these are indirect and lack sensitivity.

We measured caudate nucleus area (blind to the subject's clinical state) in 30 subjects with or at risk of Huntington's disease and in 100 normal age matched control.

Outcome is awaited in 6 CT caudate area measurement is simple and reproducible and we have found it to be a useful confirmatory test for Huntington's disease. (WardlawJM,SellarRJ,Abernethy LJ

Chapter three
Materials and method

Chapter three

Materials and method

3.1 Materials

3.1.1 Subjects:-

One hundred patient which their results are normal selected ,aged between 8 month to 73 years old.

3.1.2 Study area and duration:-

Royal care hospital and AL zaytouna hospital

Duration

3/9/2016 to 29/11/2016

3.2Method

3.2.1MRI protocol :-

Brain images where are obtained at Royal care hospital and ALZETOUNA hospital using 1.5 tesla MRI machine, Patient head were aligned along the midline using head support (standard imaging protocol), At first series of scout image (8 to 10 slices) 5mm thick with 1 mm inter slice gap, Was acquired to verify head position and image quality

3.2.2 Techinqe used

The sequence used for the measurement were coronal T2 weighted spin echo image with the following parameter

TE= 105msec

TR= 500msec

Slice thickness= 5 mm

Inter slice gap= 1mm

acquisition angle=90

The coronal T2 weighted image is highly sensitive to local pathology and provide good demarcation of the CSF containing space when results in high spatial resolution image with excellent contrast to be used for measurement by means of manual tracing of caudate nucleus structures

3.2.3 MRI processing:-

The brain images were transferred to PC workstation (using paxera viewer bundled version) that provides reliable morphometry and manual tracing after image acquisition

3.2.4 Delineation of caudate nucleus :-

The head ,body and tail of caudate nucleus was estimated on the basis of 20 coronal slices

3.2.5 Statistical analysis:-

Was performed using SPSS 22

3.2.6 Tracing method used:-

The head of caudate nucleus is the anterior portion of the nucleus. It forms that lateral wall of the anterior horn of lateral ventricle. The body of caudate nucleus is the middle portion of the caudate nucleus lying on the thalamus

The tail of caudate nucleus is the portion of the nucleus that tapers off posteroinferiorly

CHAPTER FOUR

Results

Table 4.1: Characteristics of subjects enrolled in Magnetic Resonance Imaging studies of the Caudate Nucleus:

	age	RTHL	RTBL	RTTL	RTHW	RTBW	RTTW	LTHL	LTBL	LTTL	LTHW	LTBW	LTTW
Mean	28.62	23.03	17.71	9.32	9.03	7.14	4.38	21.03	16.10	8.09	8.46	6.57	3.81
Std. Deviation	19.31	2.31	2.34	1.68	1.39	1.409	.95	2.22	2.44	1.84	1.40	1.29	1.00
Minimum	.67	17.84	11.04	5.08	5.13	3.85	2.00	16.10	10.62	4.49	5.30	3.01	1.15
Maximum	80.00	29.93	23.83	13.40	12.20	10.35	6.85	26.27	22.36	12.56	12.21	10.12	6.10

Table 4.2: Characteristics of subjects enrolled in Magnetic Resonance Imaging studies of the caudate nucleus according to age group:

Age Recoded	RTHL	RTBL	RTTL	RTHW	RTBW	RTTW	LTHL	LTBL	LTTL	LTHW	LTBW	LTTW
Mean	23.83	18.18	9.32	9.27	7.30	4.51	21.78	16.35	8.13	8.59	6.61	3.93
Std. Deviation	3.17	2.67	1.46	1.33	1.03	.85	2.85	2.76	1.76	1.42	1.26	1.03
Mean	22.94	18.09	9.15	9.57	7.61	4.55	20.89	16.50	7.93	8.73	6.89	3.75
Std. Deviation	1.80	2.00	1.78	1.16	1.36	1.00	1.87	2.17	1.86	1.36	1.04	.85
Mean	23.11	17.22	9.24	8.77	7.22	4.33	21.00	15.86	8.01	8.37	6.61	3.94
Std. Deviation	1.68	1.97	2.07	1.38	1.36	.98	1.47	2.35	1.97	1.13	1.17	1.02
Mean	22.08	16.51	9.41	8.42	6.22	3.96	20.46	15.43	8.23	7.98	6.11	3.52
Std. Deviation	1.45	2.60	1.38	1.46	1.69	.88	2.22	2.17	2.14	1.32	1.57	.96
Mean	21.70	18.18	10.59	7.78	6.16	4.35	19.64	16.21	8.63	8.36	6.05	3.82
Std. Deviation	1.59	2.38	1.39	1.16	1.39	.83	1.62	2.38	1.52	2.16	1.99	1.76
Mean	23.06	17.71	9.33	9.06	7.16	4.40	21.06	16.15	8.08	8.49	6.59	3.81
Std. Deviation	2.30	2.36	1.69	1.37	1.39	.93	2.22	2.39	1.85	1.37	1.27	1.00

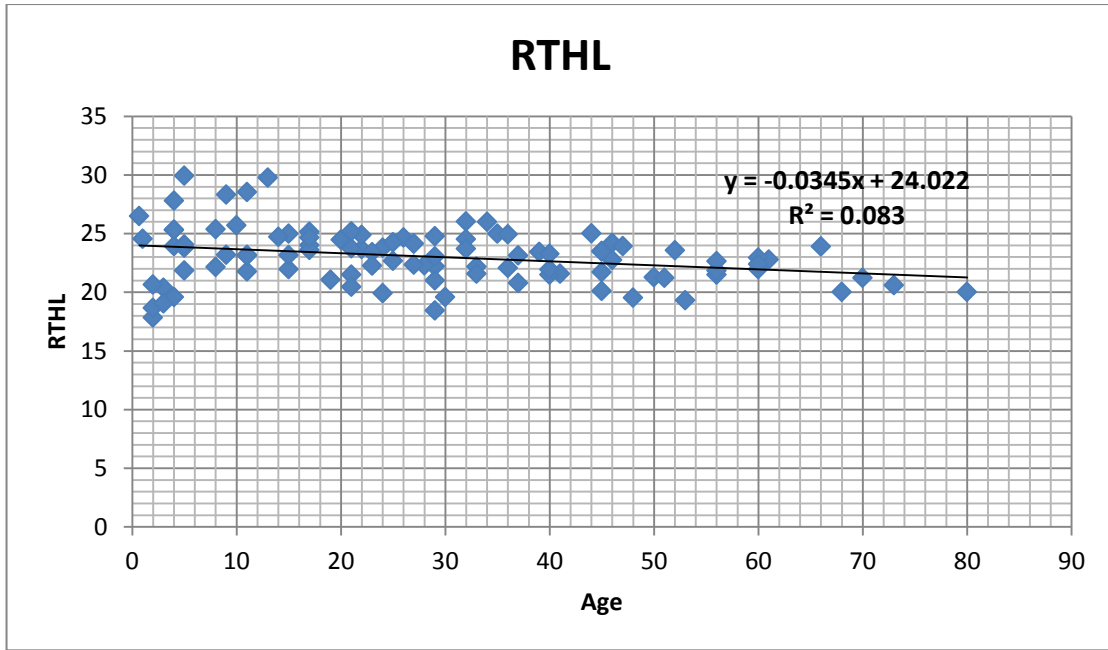


Figure 4.1 A scatter plot diagram shows relationship between the **RTHL** and the **Age** of the subjects, $R^2=0.083$.

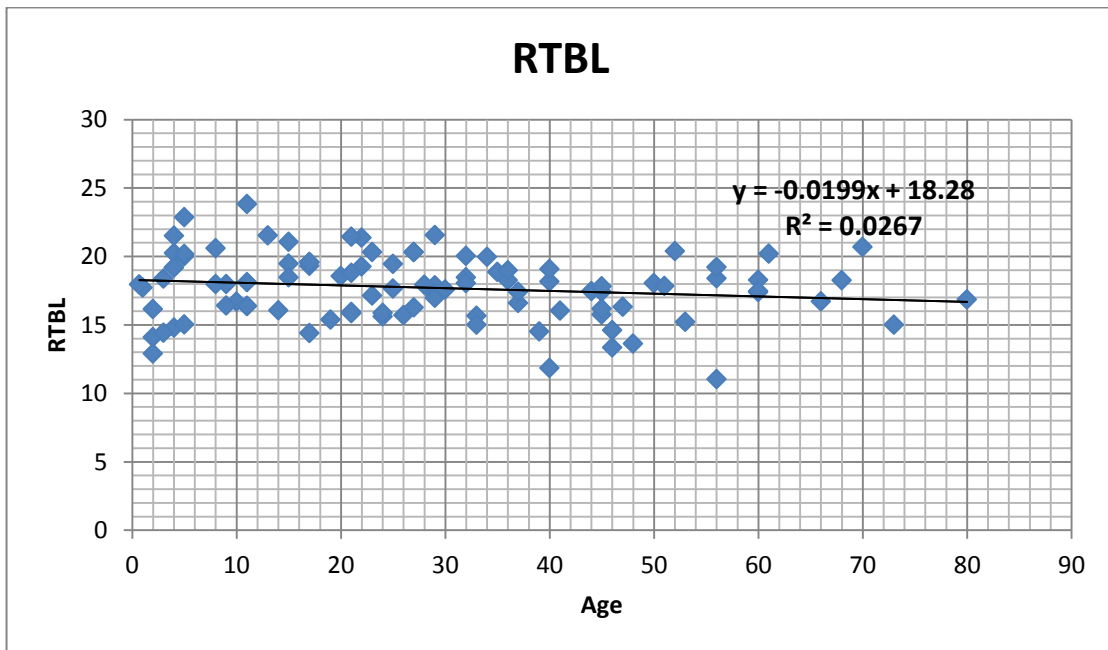


Figure 4.2 A scatter plot diagram shows relationship between the **RTBL** and the **Age** of the subjects, $R^2=0.026$.

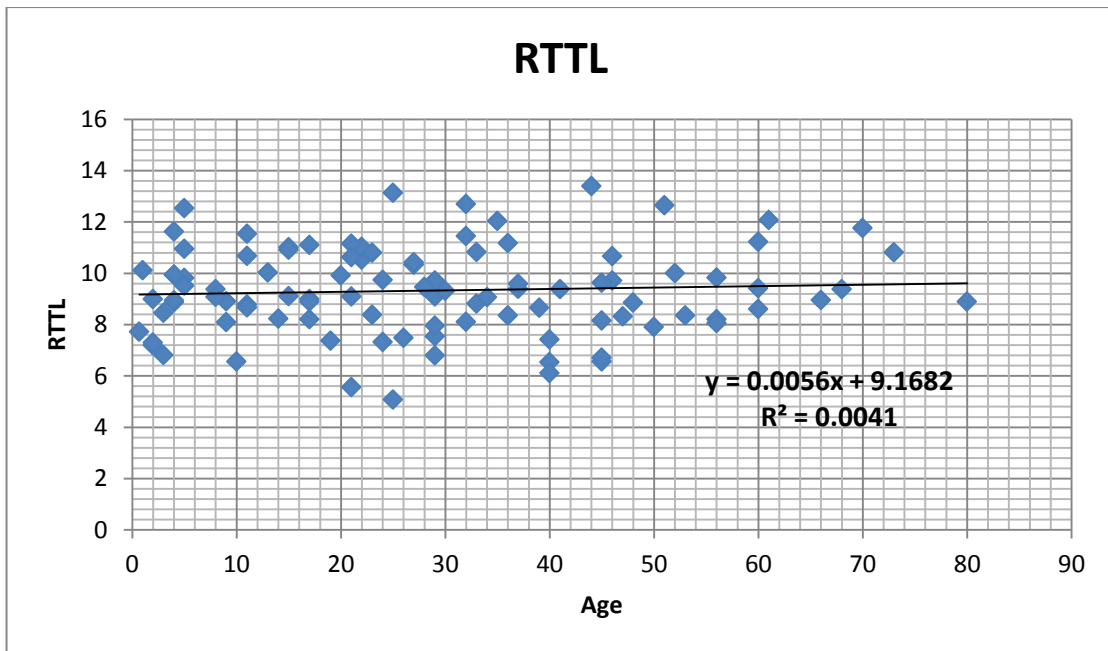


Figure 4.3 A scatter plot diagram shows relationship between the **RTTL** and the **Age** of the subjects, $R^2=0.004$.

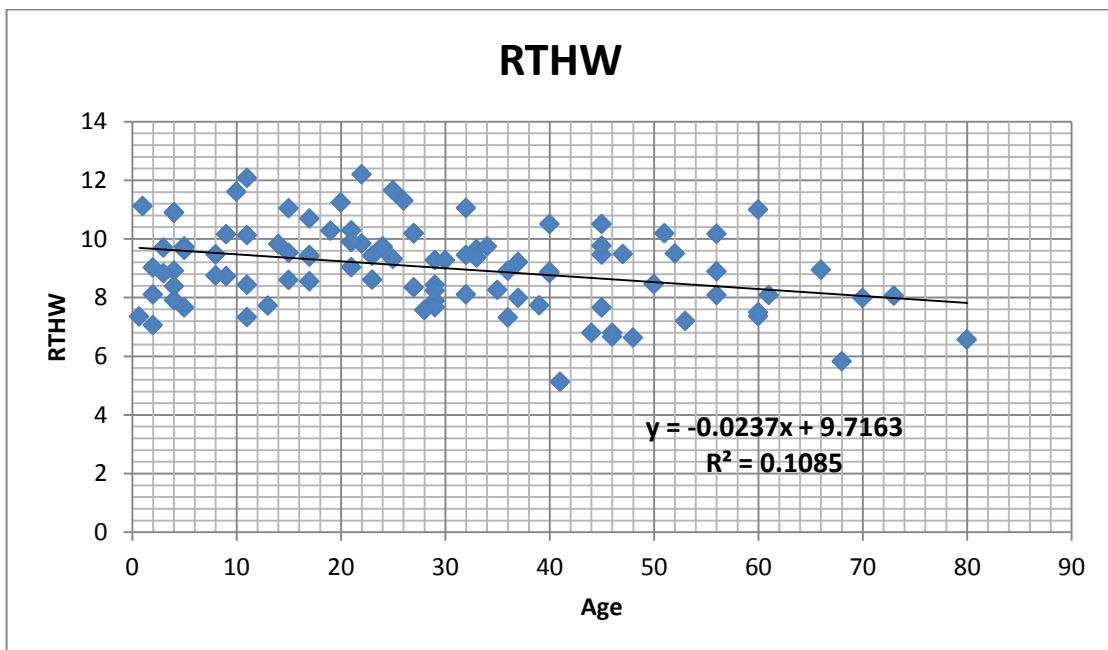


Figure 4.4 A scatter plot diagram shows relationship between the **RTHW** and the **Age** of the subjects, $R^2=0.108$.

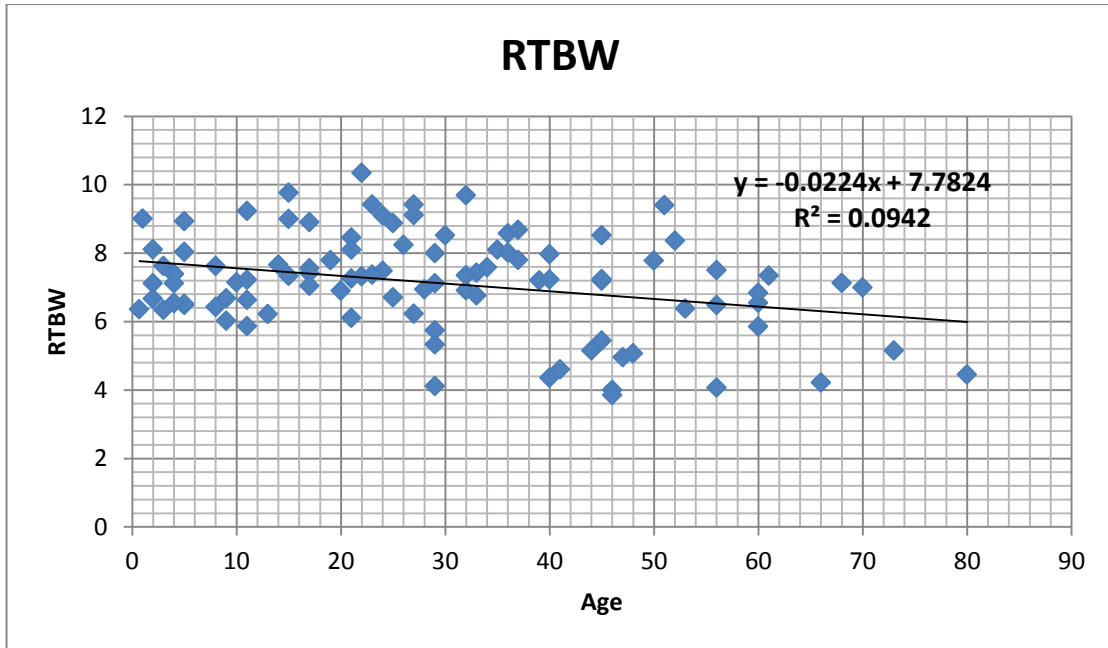


Figure 4.5 A scatter plot diagram shows relationship between the **RTBW** and the **Age** of the subjects, $R^2=0.094$.

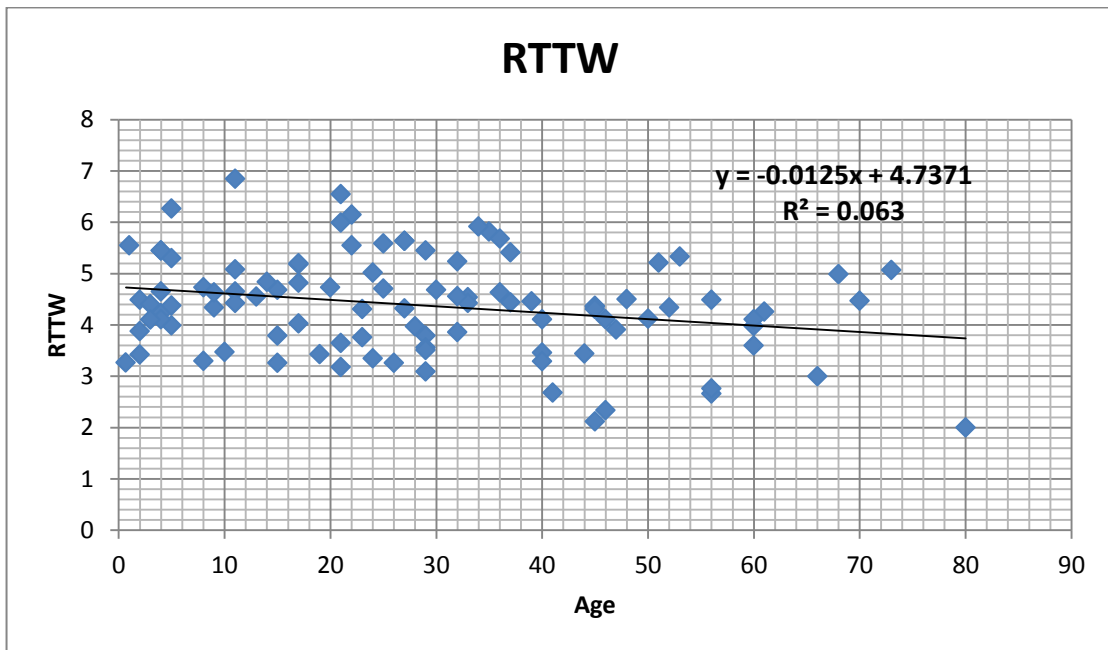


Figure 4.6 A scatter plot diagram shows relationship between the **RTTW** and the **Age** of the subjects, $R^2=0.063$.

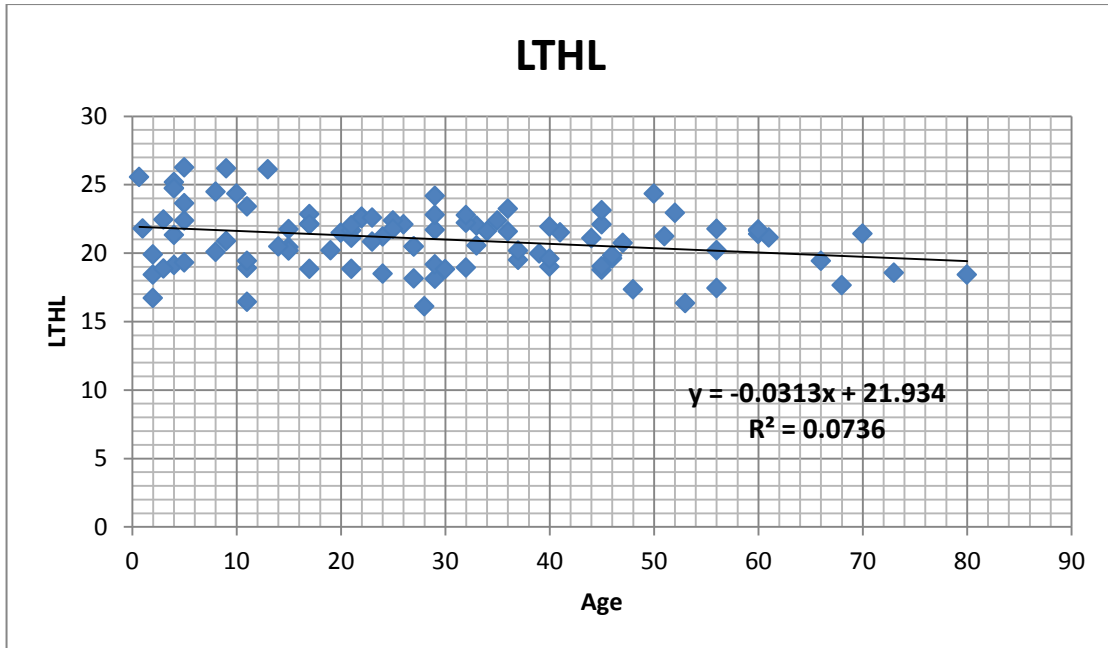


Figure 4.7 A scatter plot diagram shows relationship between the **RTHL** and the **Age** of the subjects, $R^2=0.073$.

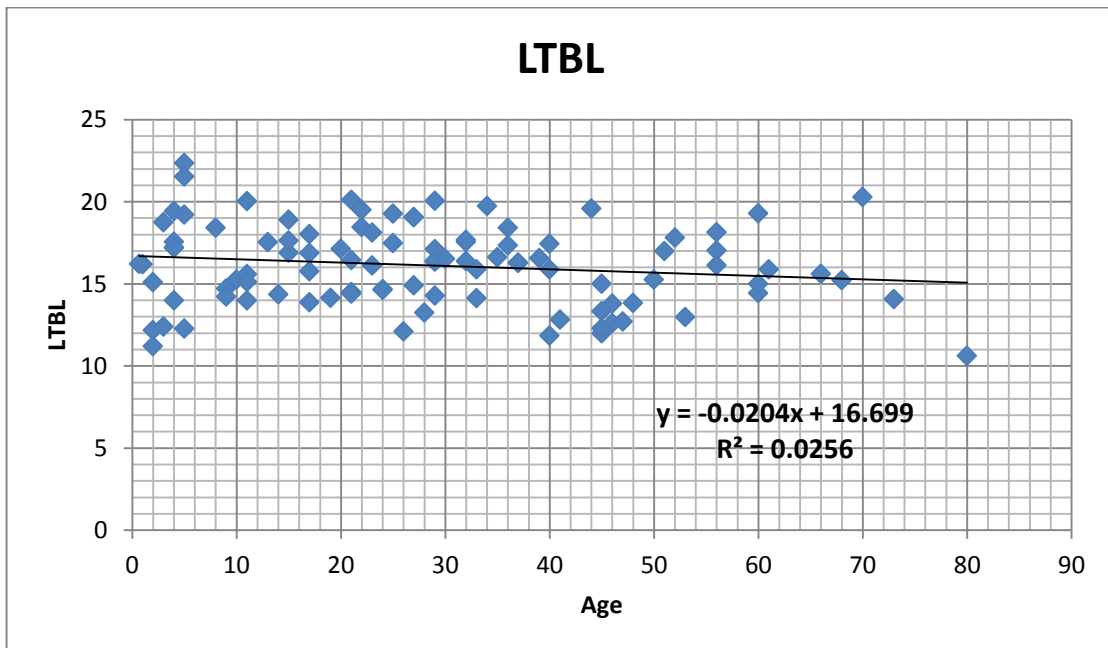


Figure 4.8 A scatter plot diagram shows relationship between the **LTBL** and the **Age** of the subjects, $R^2=0.025$.

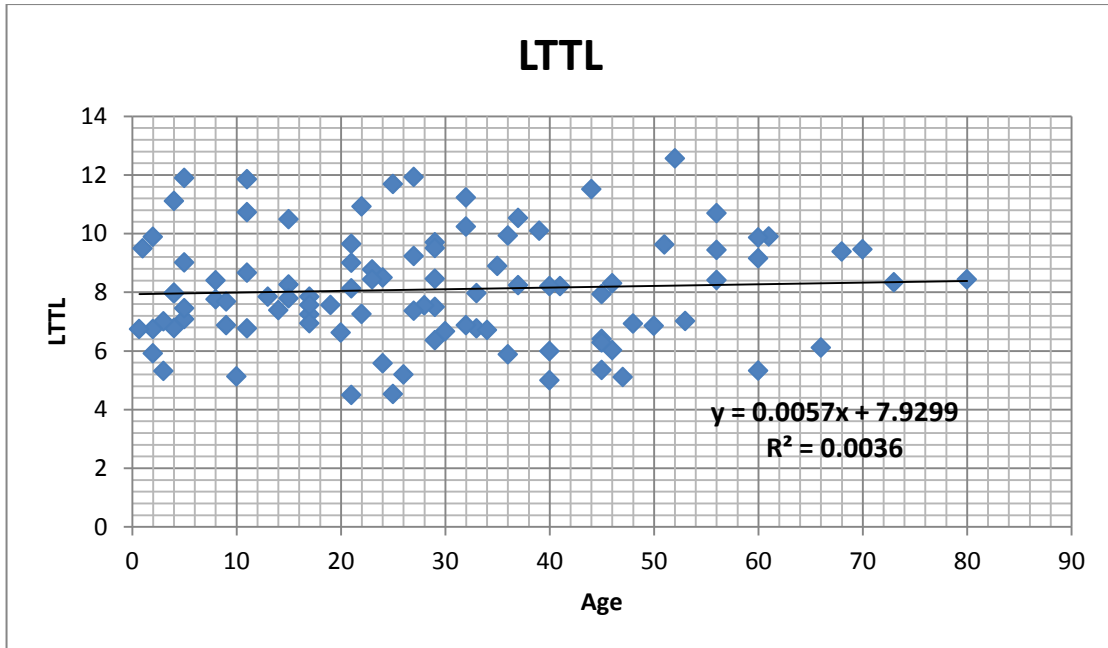


Figure 4.9 A scatter plot diagram shows relationship between the **LTTL** and the **Age** of the subjects, $R^2=0.003$.

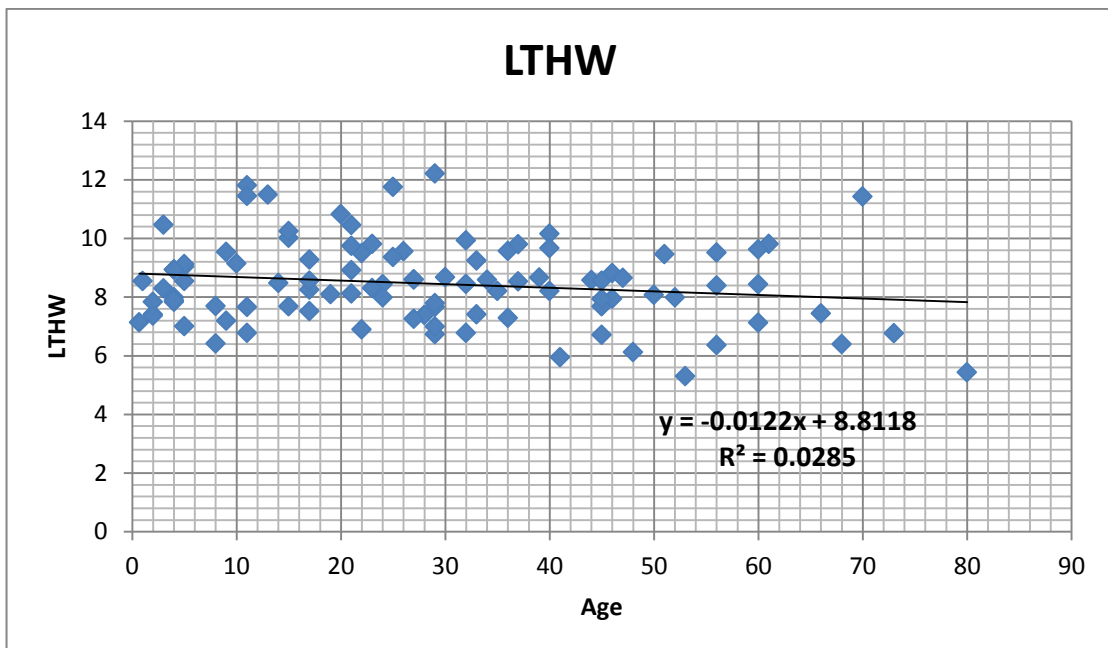


Figure 4.10 A scatter plot diagram shows relationship between the **LTHW** and the **Age** of the subjects, $R^2=0.028$

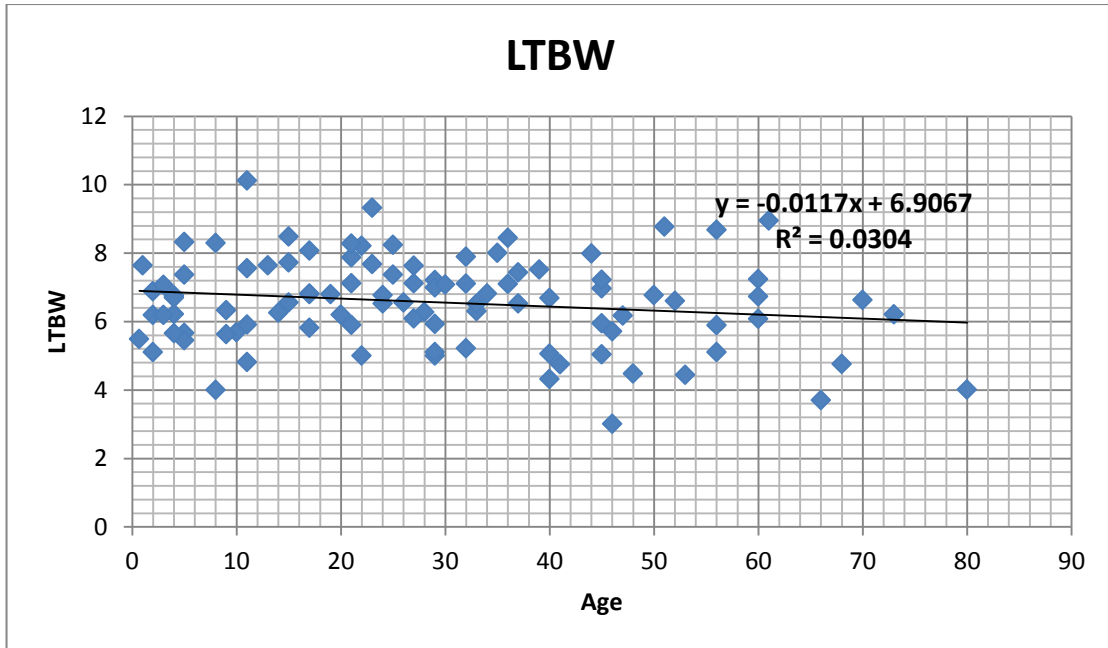


Figure 4.11 A scatter plot diagram shows relationship between the **LTBW** and the **Age** of the subjects, $R^2=0.030$

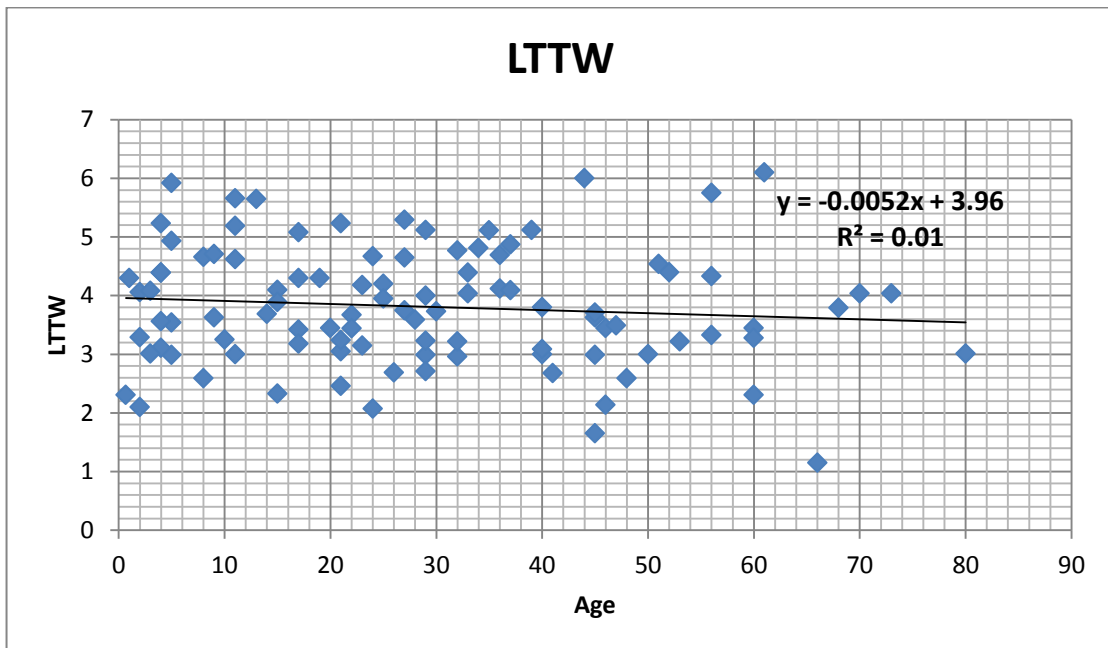


Figure 4.12 A scatter plot diagram shows relationship between the **LTTW** and the **Age** of the subjects, $R^2=0.01$.

Table 4.3 comparison between males and females:

	gender	age	RTHL	RTBL	RTTL	RTHW	RTBW	RTTW	LTHL	LTBL	LTTL	LTHW	LTBW	LTW
Mean	M	27.82	23.45	18.18	9.60	9.16	7.18	4.31	21.26	16.40	8.34	8.44	6.58	3.82
Mean	F	29.43	22.61	17.23	9.05	8.90	7.10	4.44	20.81	15.79	7.84	8.48	6.55	3.80

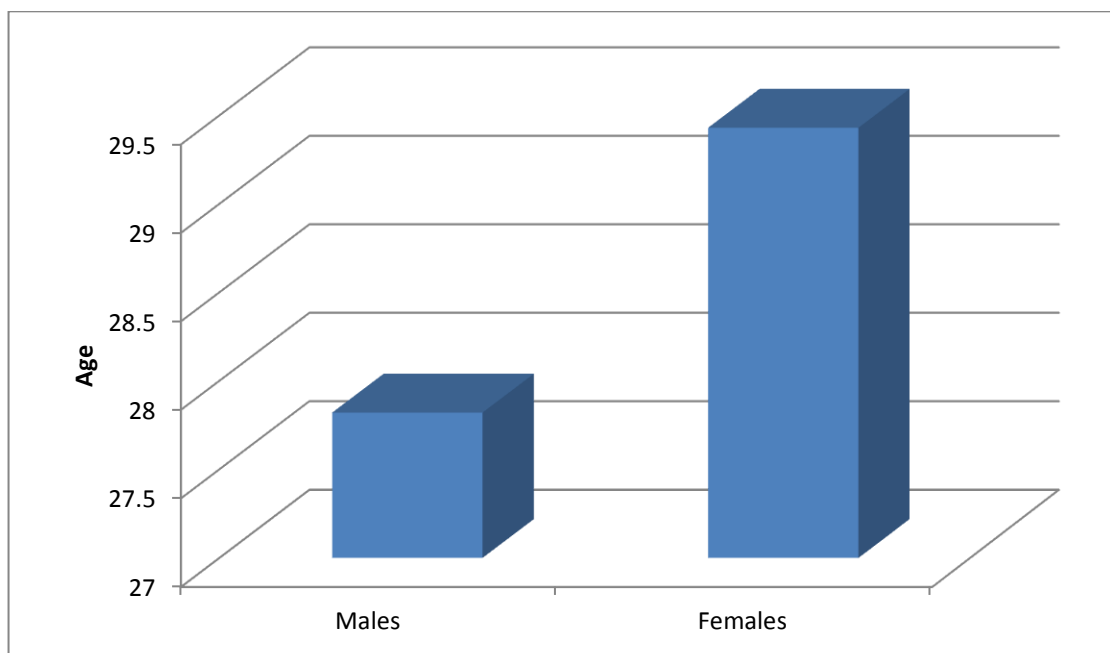


Fig 4.13: comparison between males and females in mean Age

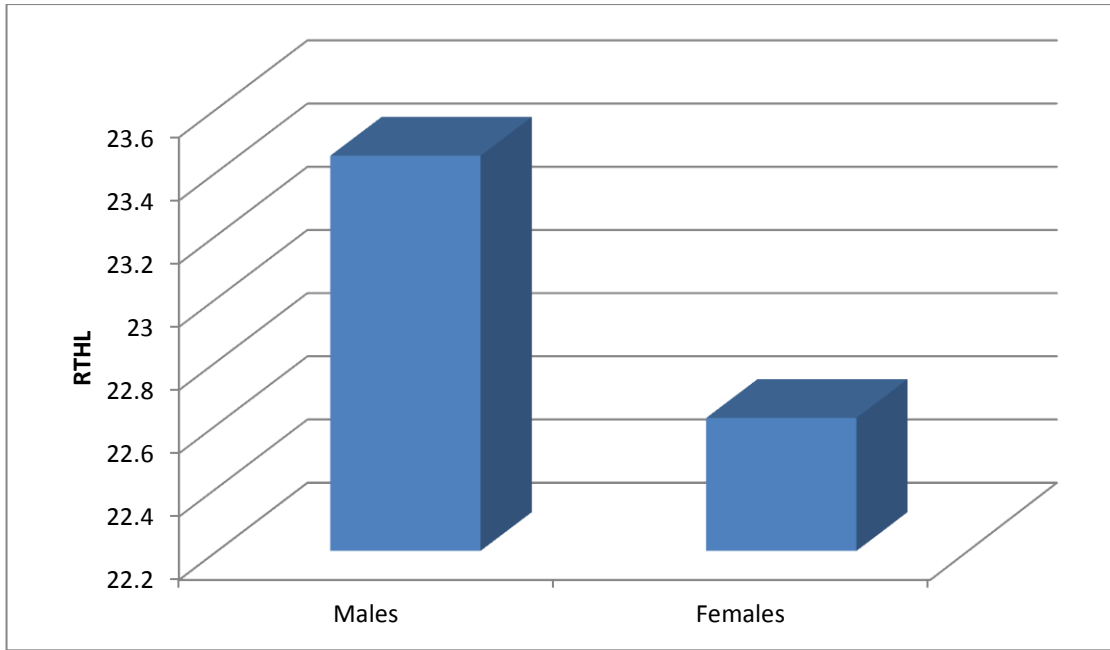


Fig 4.14: comparison between males and females in **RTHL**

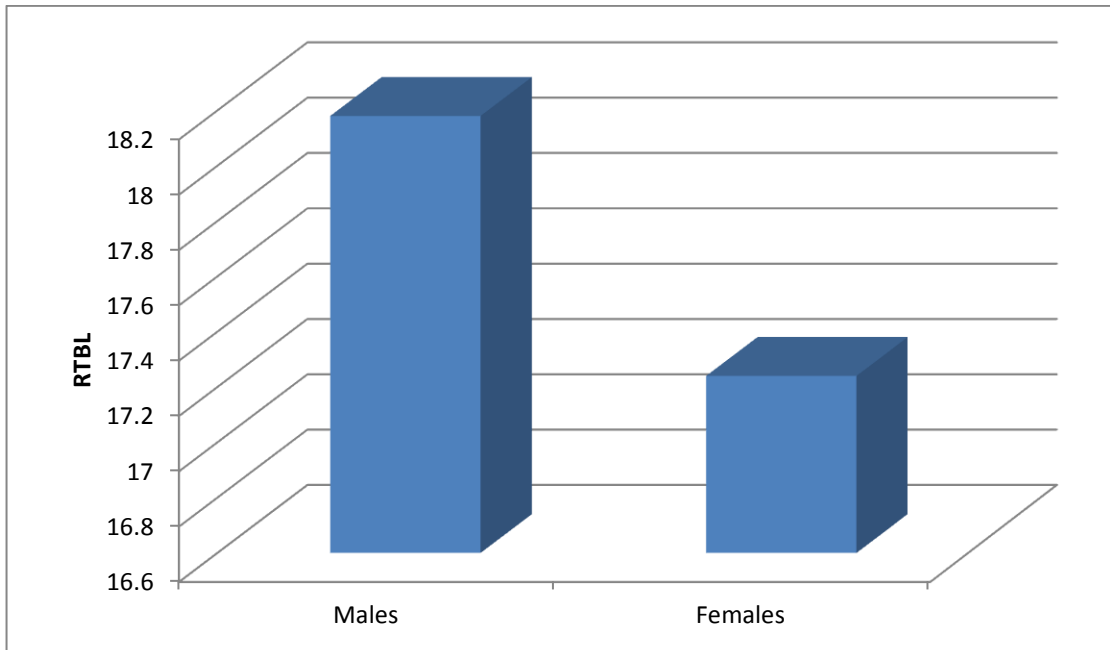


Fig 4.15: comparison between males and females in **RTBL**.

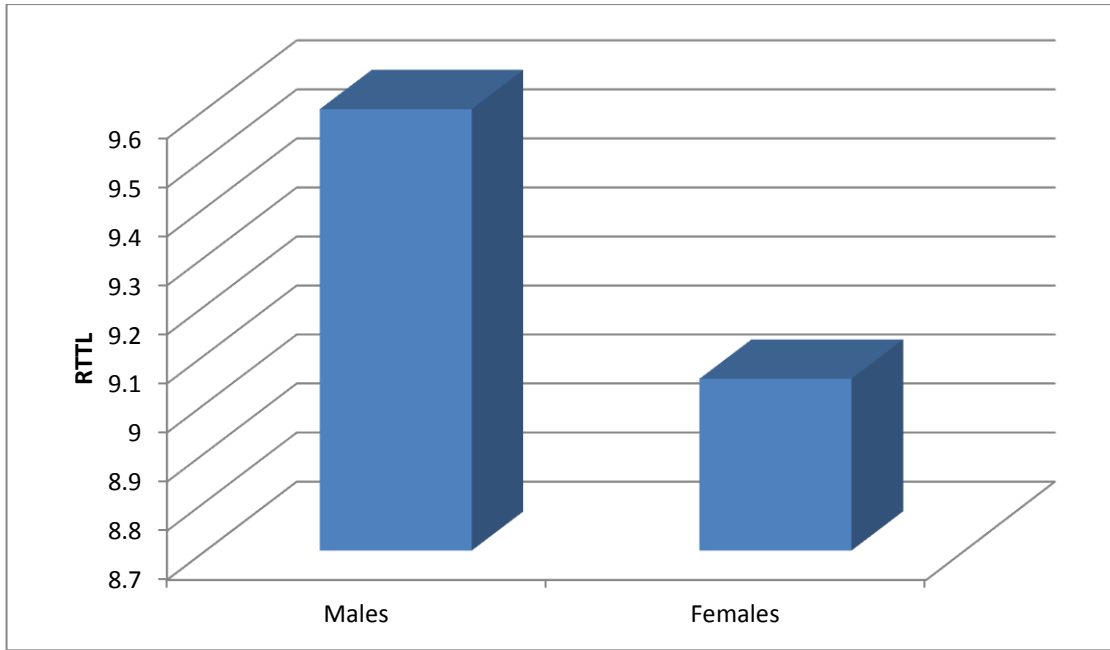


Fig 4.16: comparison between males and females in **RTTL**.

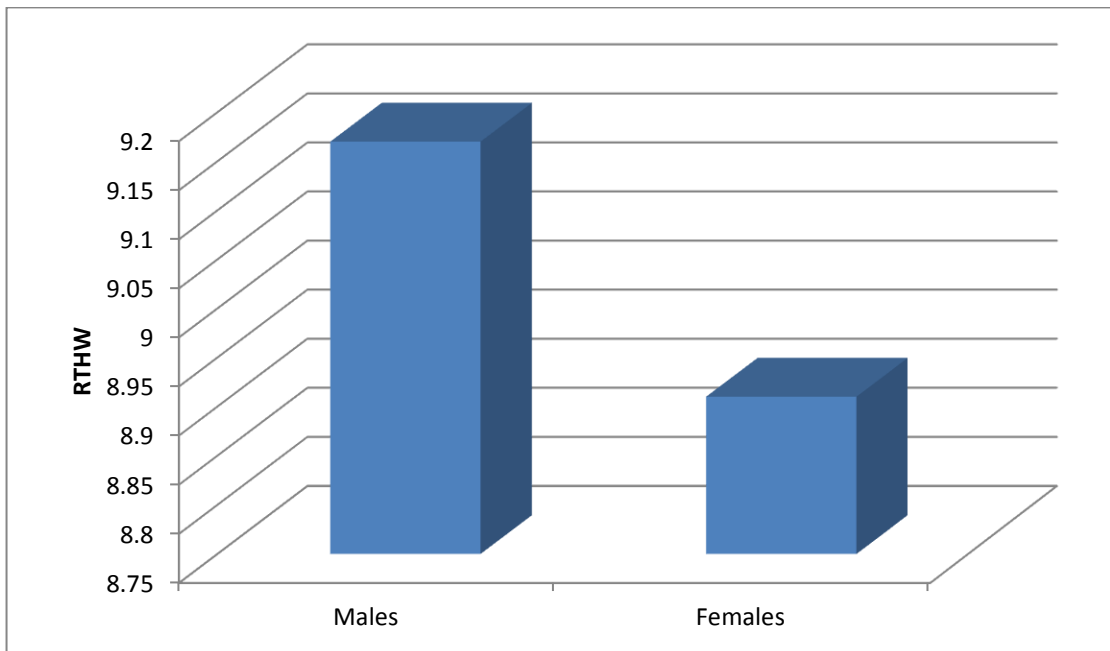


Fig 4.17: comparison between males and females in **RTHW**.

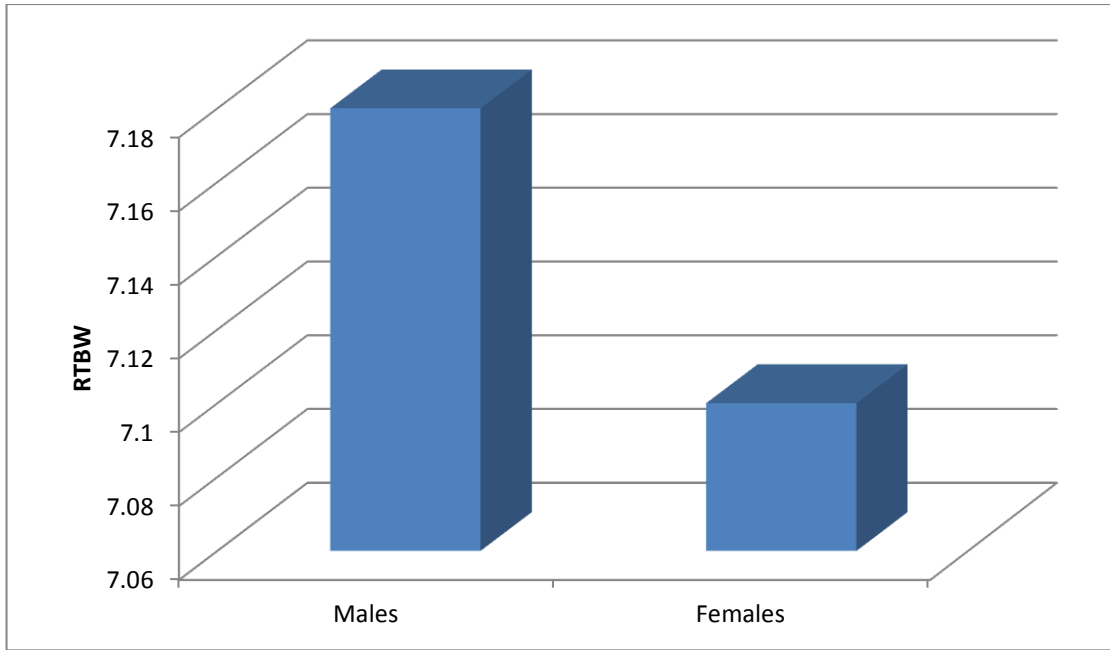


Fig 4.18: comparison between males and females in **RTBW**

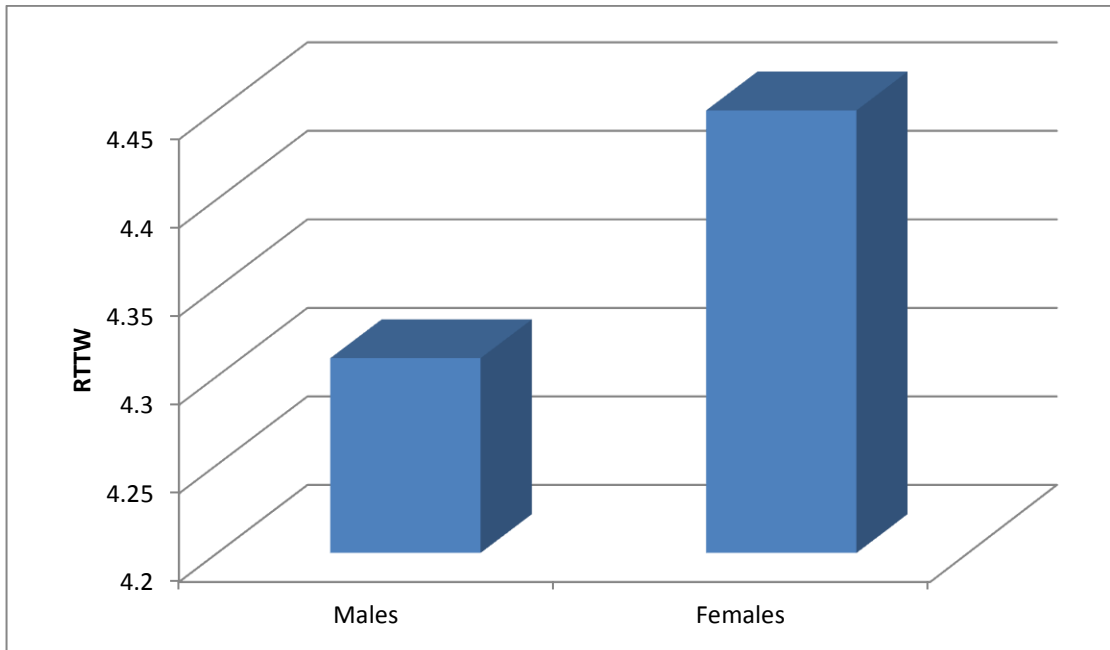


Fig 4.19: comparison between males and females in **RTTW**

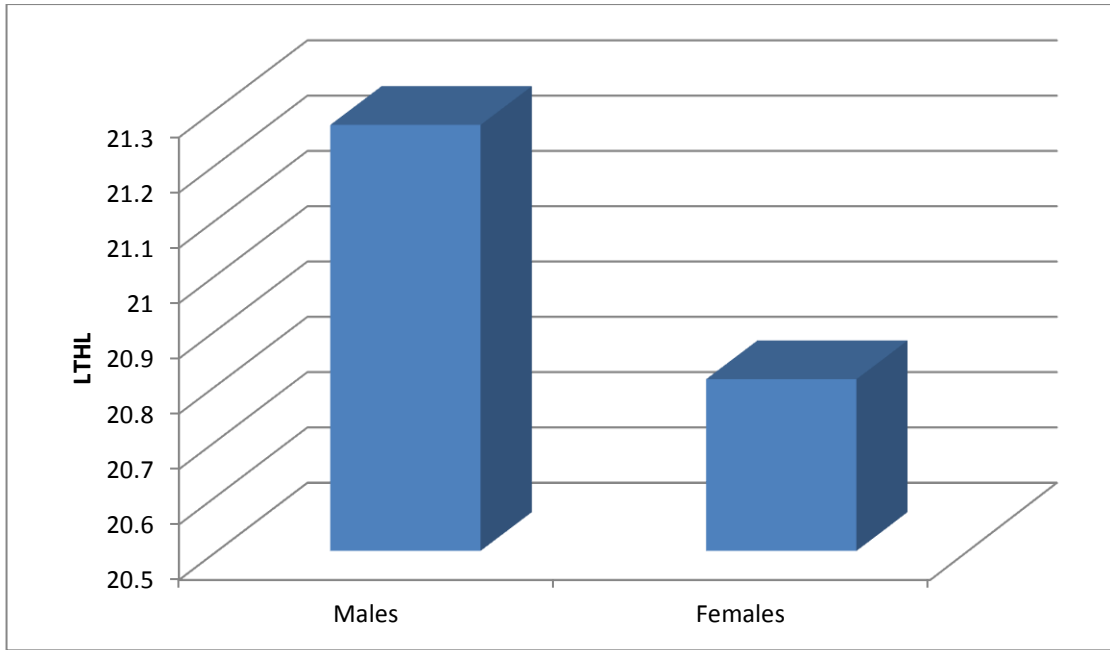


Fig 4.20: comparison between males and females in **LTHL**.

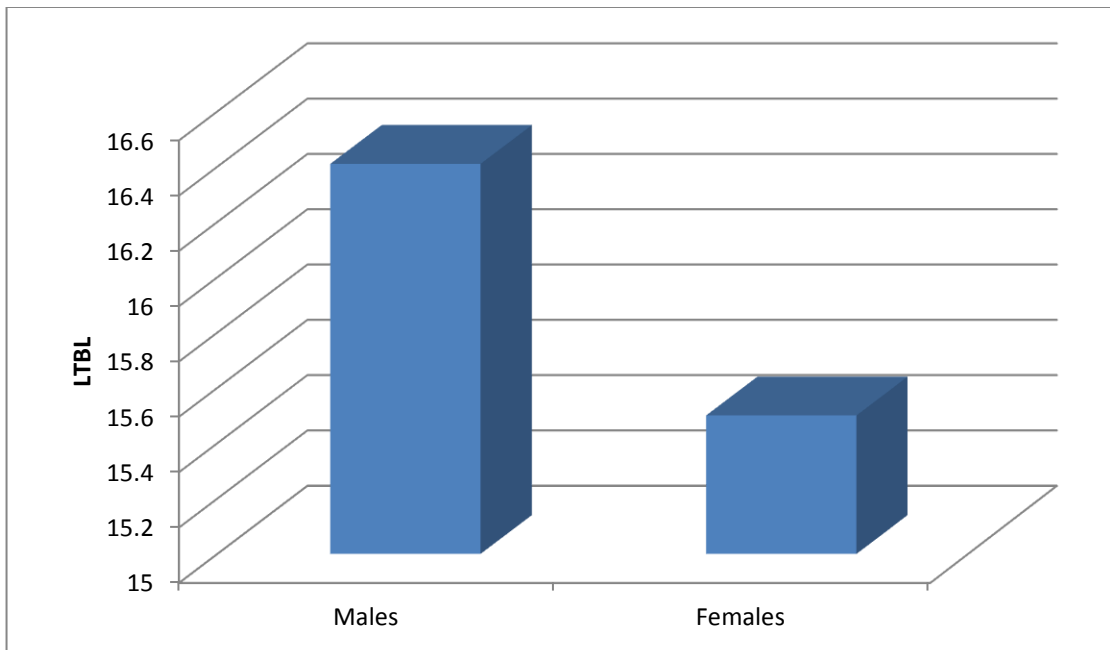


Fig 4.21: comparison between males and females in **LTBL**.

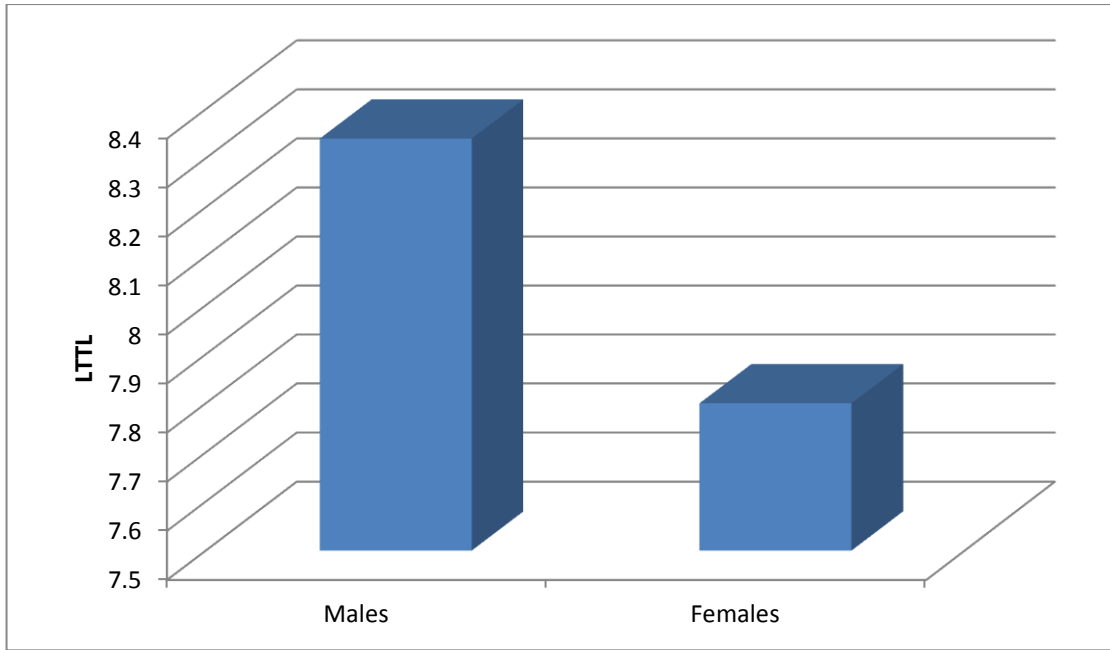


Fig 4.22: comparison between males and females in **LTTL**.

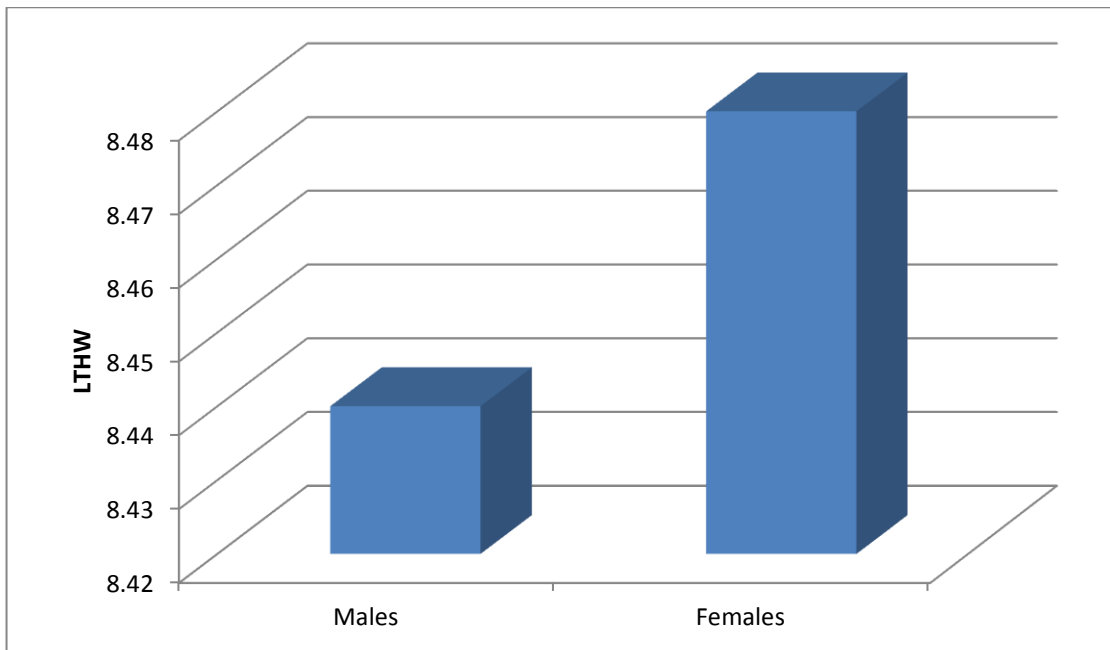


Fig 4.23: comparison between males and females in **LTHW**

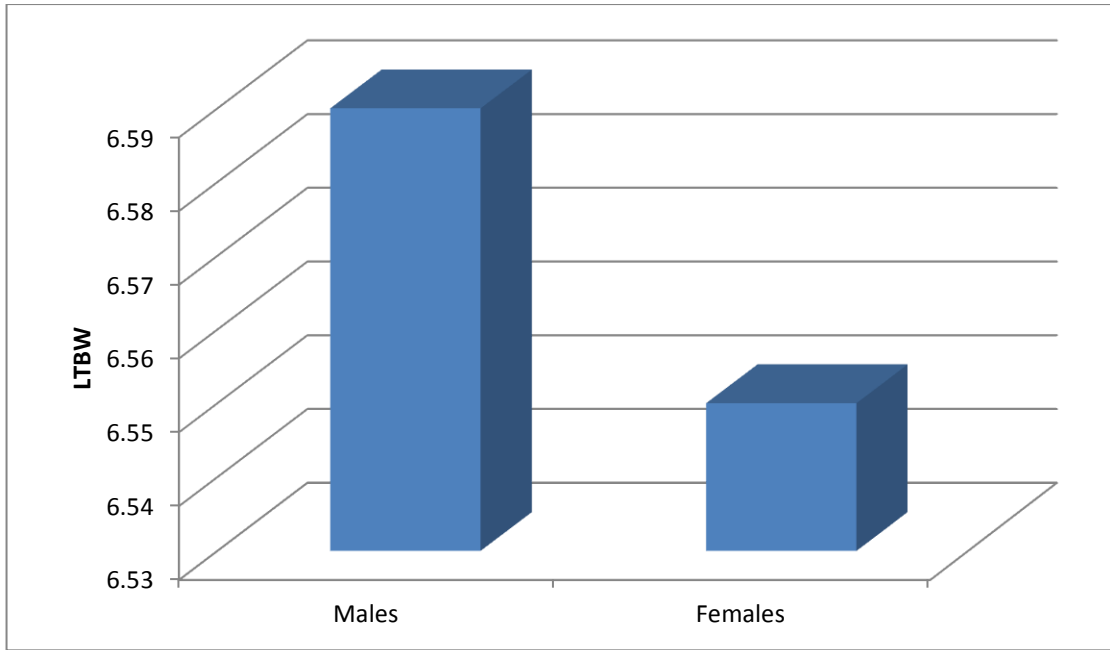


Fig 4.24: comparison between males and females in **LTBW**.

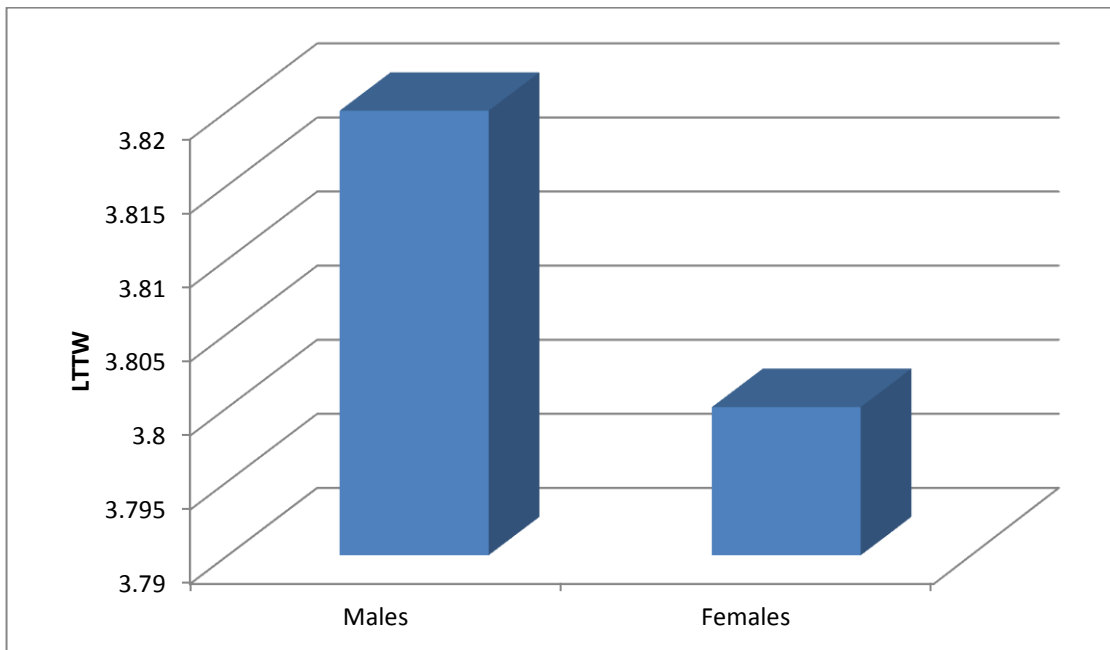


Fig 4.25: comparison between males and females in **LTTW**.

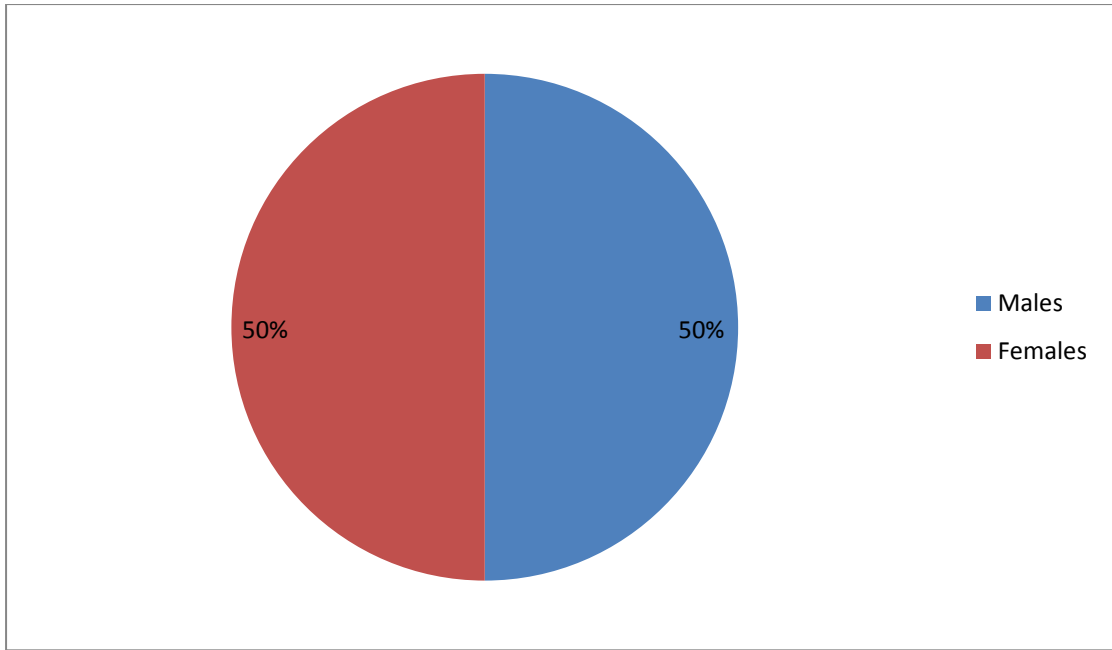


Fig 4.26:total number of patient(100)

Chapter Five

Discussion, Conclusion and Recommendations

5.1 Discussion:

The objective of this study was to measure the length and width caudate nucleus in normal Sudanese population in magnetic resonance imaging (MRI) and age related differences. This study was performed on 100 patients. The data collected from patients of ages ranged between 8 months-73 years old.

The study found that the mean of length and width of the right and left head and body and tail of caudate nucleus for total population were

RTHL 23.03, RTBL 17.71, RTTL 9.32, RTHW 9.03, RTBW 7.14, RTTW 4.38, LTHL 21.03, LTBL 16.10, LTTL 8.09, LTHW 8.46, LTBW 6.57, LTTW 3.81 in mm

and the mean for the length and width of the right and left head and body and tail of caudate nucleus for males and females were Length in males RTHL 23.45, RTBL 18.18, RTTL 9.60, LTHL 21.26, LTBL 16.40, LTTL 8.34

Width in males RTHW 9.16, RTBW 7.18, RTTW 4.31, LTHW 8.44, LTBW 6.58, LTTW 3.82

Length in females RTHL 22.61, RTBL 17.23, RTTL 9.05, LTHL 20.81, LTBL 15.79, LTTL 7.84

Width in females RTHW 8.90, RTBW 7.10, RTTW 4.44, LTHW 8.48, LTBW 6.55, LTTW 3.80 In mm

A significant negative correlation was observed between right head length of caudate and Age for total population ($r = -0.083$) (Fig 4.1)

A significant negative correlation was observed between right body length of caudate and Age for total population ($r = -0.026$) (Fig 4.2)

A significant positive correlation was observed between right tail length of caudate and Age for total population ($r = -0.004$) (Fig 4.3)

A significant negative correlation was observed between right head width of caudate and Age for total population ($r = -0.108$) (Fig 4.4)

A significant negative correlation was observed between right body width of caudate and Age for total population ($r = -0.094$) (Fig 4.5)

A significant negative correlation was observed between right tail width of caudate and Age for total population ($r = -0.063$) (Fig 4.6)

A significant negative correlation was observed between left head length of caudate and Age for total population ($r = -0.073$) (Fig 4.7)

A significant negative correlation was observed between left body length of caudate and Age for total population ($r = -0.025$) (Fig 4.8)

A significant positive correlation was observed between left tail length of caudate and Age for total population ($r = 0.003$) (Fig 4.9)

A significant negative correlation was observed between left head width of caudate and Age for total population ($r = -0.028$) (Fig 4.10)

A significant negative correlation was observed between left body width of caudate and Age for total population ($r = -0.030$) (Fig 4.11)

A significant negative correlation was observed between left tail width of caudate and Age for total population ($r = -0.01$) (Fig 4.12)

At the age of 40 the length and width start to decrease .except in fig 4.3 & 4.9

The mean age for females was 29.43 years old and the mean age for males was 27.82 years old

The mean in females was higher than males by 1.61 years ,

the mean length value of right and left head of caudate nucleus in male was larger than in females by (RT + 0.84/LT + 0.45) mm respectively

the mean width value of right and head of caudate nucleus in male was larger than in females by (RT + 0.26) mm respectively but the mean width value of left head of caudate nucleus in females was larger than in males by (LT + 0.04) mm respectively

the mean length value of right and left body of caudate nucleus in male was larger than in females by (RT + 0.95/LT + 0.61) mm respectively

the mean width value of right and left body of caudate nucleus in male was larger than in females by (RT + 0.08/LT + 0.03) mm respectively

the mean length value of right and left tail of caudate nucleus in male was larger than in females by (RT + 0.55/LT +0.5) mm respectively

the mean width value of right and left tail of caudate nucleus in male was larger than in females by (RT + 0.13/LT +0.02)mm respectively

These measurements were compared to study done Journal of Paramedical Sciences (JPS) Spring 2013 Vol.4, No.2 ISSN 2008-4978

The results of the statistical analysis on age related changes for both sides of the caudate and putamen volumes . There exist significant negative correlations between age and caudate volume in male group (right side: $r=-0.718$, $P<0.001$; left side: $r=0.721$, $P<0.001$). In female group, there exist significant negative correlations between age and caudate volume (right side: $r=-0.627$, $P<0.001$; left side: $r=-0.569$, $P<0.001$).

This difference may be due to racial differences and patient habits.

Conclusion

We concluded that According to the normal cells adaptation the age have direct effect on the caudate nucleus size and noted that increase age lead to decrease caudate nucleus , also the size of the caudate nucleus is higher in male than female.

Recommendations:-

Further study in evaluation of caudate nucleus with larger sample of Sudanese population for more accurate results is needed.

Future studies should calculate the caudate nucleus volume to give full demographic information

References

Ali Abedelahi, HadiHasanzadeh (2013), MRI Dased Morphometry of Caudate Nucleus in Normal Persons, Journal of Paramedical Sciences (JPS), Vol.4, No 2,ISSN 2008-4987

Aylward EH, Rosenblatt A, Field K, Yallapragada V, Kieburtz K, McDermott M, et al. Caudate volume as an outcome measure in clinical trials for Huntington's disease: a pilot study. Brain research bulletin. 2003;62(2):137-41. Epub 2003/11/26

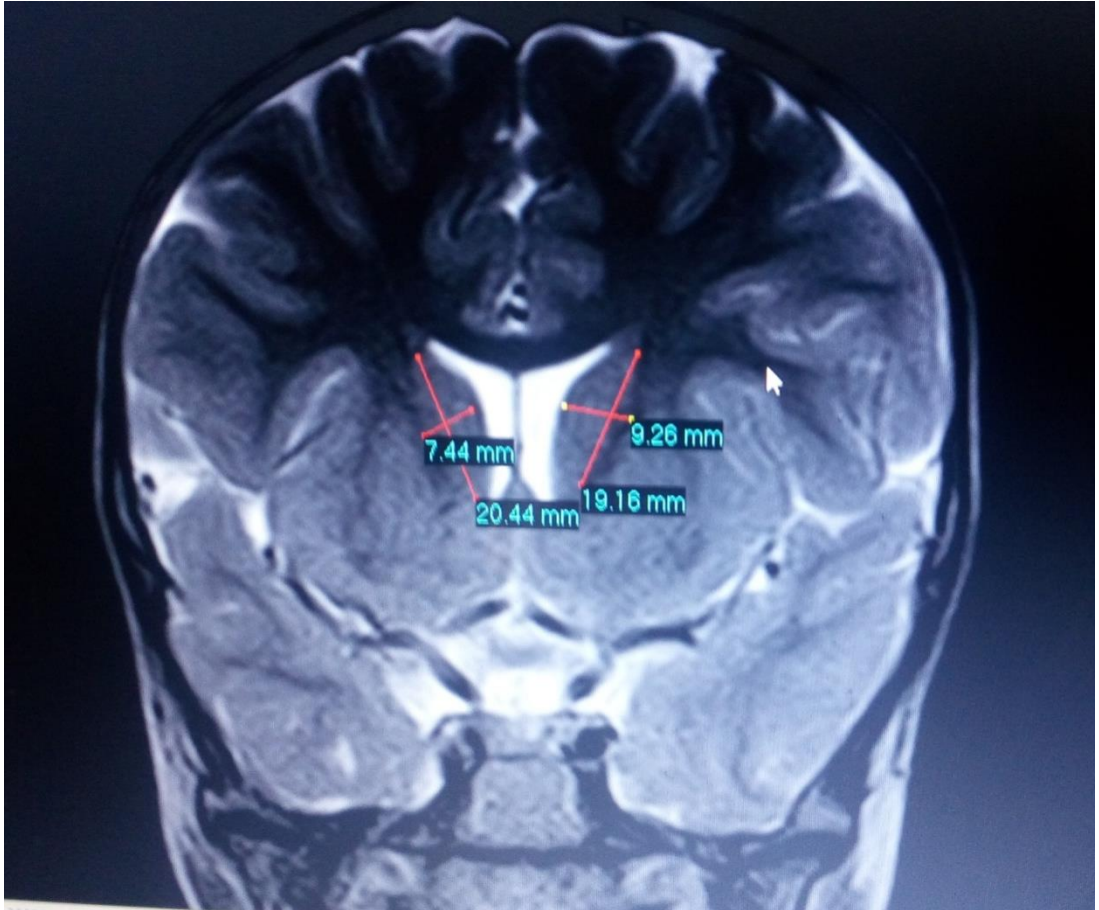
Corson PW, Nopoulos P, Andreasen NC, Heckel D, Arndt S. Caudate size in first-episode neuroleptic-naive schizophrenic patients measured using an artificial neural network. Biological psychiatry. 1999;46(5):712-20. Epub 1999/09/03.

Ferrarini L, Palm WM, Olofsen H, van Buchem MA, Reiber JH, Admiraal-Behloul F. Shape differences of the brain ventricles in Alzheimer's disease. NeuroImage. 2006;32(3):1060-9. Epub 2006/07/15.

Filipovic BR, Djurovic B, Marinkovic S, Stijak L, Aksic M, Nikolic V, et al. Volume changes of corpus striatum, thalamus, hippocampus and lateral ventricles in posttraumatic stress disorder (PTSD) patients suffering from headaches and without therapy. Central European neurosurgery. 2011;72(3):133-7. Epub 2010/09/22.

Greco PG, Meisel RL, Heidenreich BA, Garris PA. Voltammetric measurement of electrically evoked dopamine levels in the striatum of the anesthetized Syrian hamster. Journal of neuroscience methods. 2006;152(1-2):55-64. Epub 2005/09/24.

Appendices(1)



Image(1) Coronal T2 MRI Brain (head of caudate nucleus)

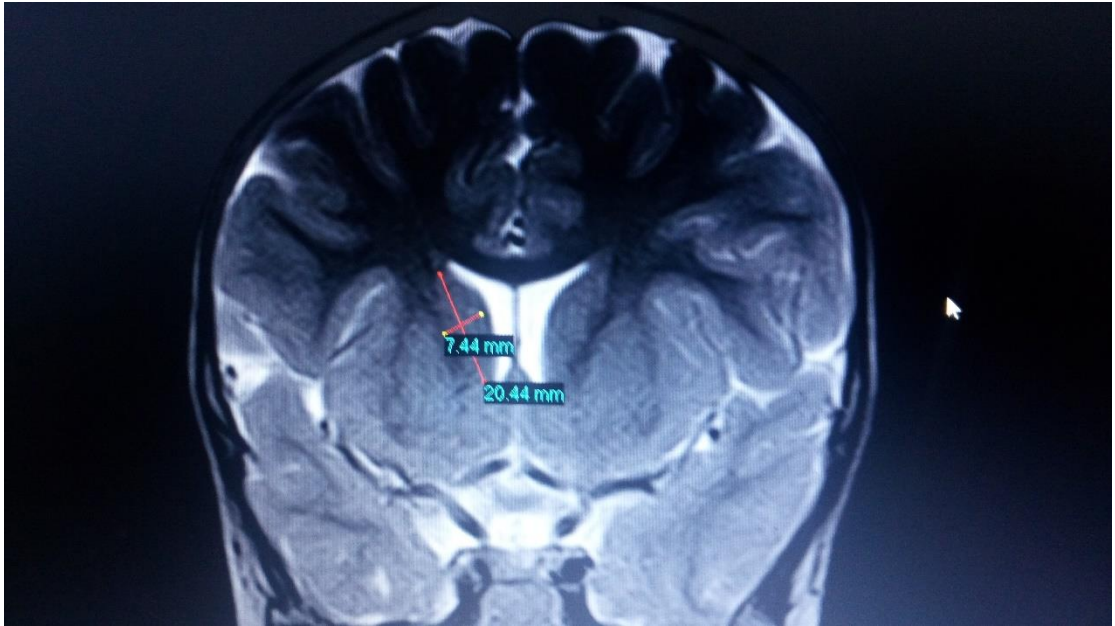
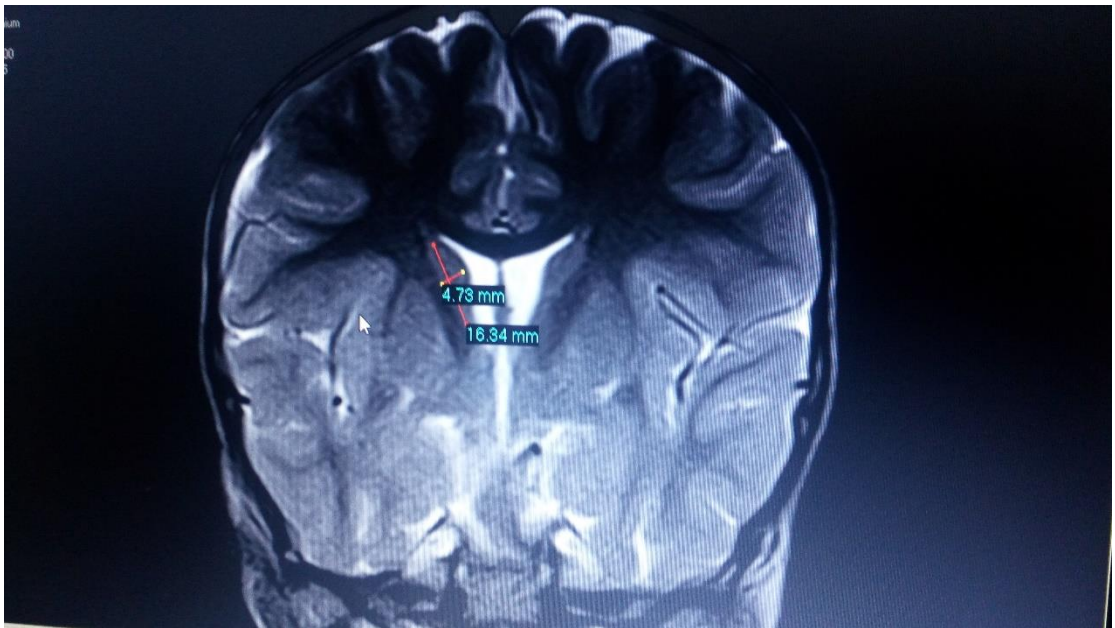


Image (2) Coronal T2 MRI Brain (head of caudate nucleus)



Image(3) coronal T2 MRI Brain (body of caudate nucleus)

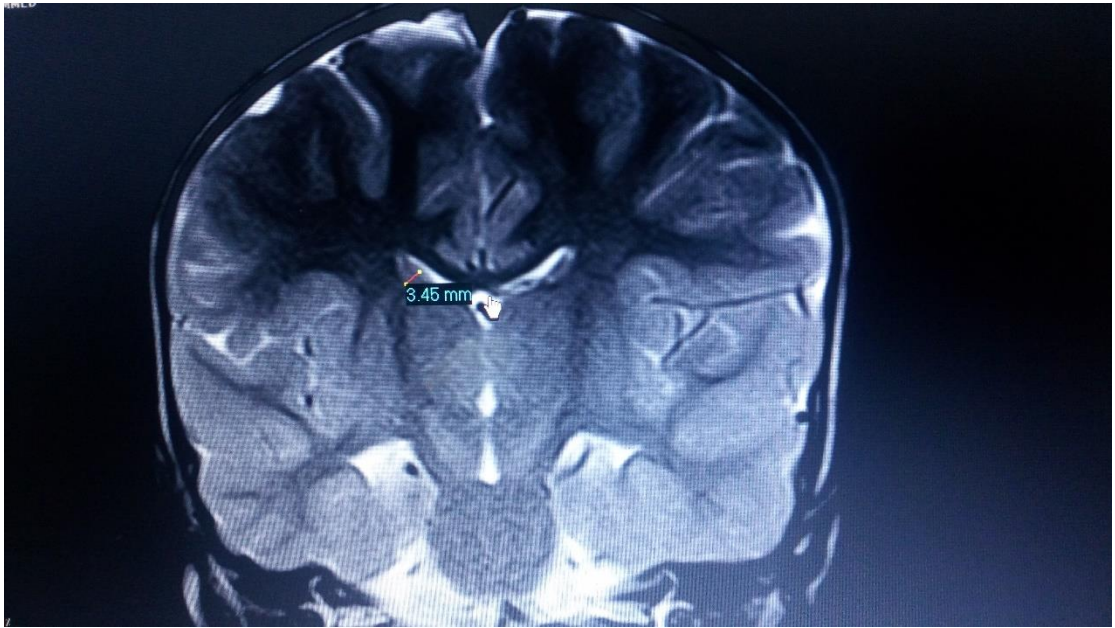


Image (4) Coronal T2 MRI Brain (tail of caudate nucleus)

